UNIVERSITY OF GAZİANTEP
GRADUATE SCHOOL OF
NATURAL & APPLIED SCIENCES

RHEOLOGICAL PROPERTIES OF ENGINEERED CEMENTITIOUS COMPOSITES CONTAINING FLY ASH

M. Sc. THESIS
IN
CIVIL ENGINEERING

BY
ZAFER BİLİCİ
DECEMBER 2011

Rheological Properties of Engineered Cementitious Composites Containing Fly Ash

M.Sc. Thesis
in
Civil Engineering
University of Gaziantep

Supervisor
Assoc. Prof. Dr. Mustafa ŞAHMARAN
Co-Supervisor
Asst. Prof. Dr. Erdoğan ÖZBAY

by
Zafer BİLİCİ
December 2011

PLAGIARISM

I hereby declare that all information in this document has been obtained and presented in accordance with academic rules and ethical conduct. I also declare that, as required by these rules and conduct, I have fully cited and referenced all material and results that are not original to this work.

Zafer BİLİCİ

Signature :

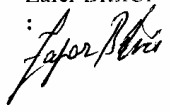

UNIVERSITY OF GAZİANTEP
GRADUATE SCHOOL OF
NATURAL & APPLIED SCIENCES
CIVIL ENGINEERING DEPARTMENT

Name of the thesis : Rheological Properties of Engineered Cementitious Composites Containing Fly Ash
Name of the student : Zafer BİLİCİ
Exam date : December 21, 2011

Approval of the Graduate School of Natural and Applied Sciences

Prof. Dr. Ramazan KOÇ
Director

I certify that this thesis satisfies all the requirements as a thesis for the degree of Master of Science.

Assoc. Prof. Dr. Mustafa GÜNAL
Head of Department

This is to certify that we have read this thesis and that in our opinion it is fully adequate, in scope and quality, as a thesis for the degree of Master of Science.

Assoc. Prof. Dr. Mustafa ŞAHMARAN
Supervisor

Assist. Prof. Dr. Erdoğan ÖZBAY
Co-Supervisor

Examining Committee Members	Signature
Assoc Prof Dr. Aytaç GÜVEN	
Assist. Prof. Dr. Hüsnü UĞUR	
Assoc. Prof. Dr. Mustafa ŞAHMARAN	

ABSTRACT

RHEOLOGICAL PROPETIES OF ENGINEERED CEMENTITIOUS COMPOSITES CONTAINING FLY ASH

BİLİCİ, Zafer
M.Sc. in Civil Engineering
Supervisor: Assoc. Prof. Dr. Mustafa ŞAHMARAN
Co-Supervisor Asst. Prof. Dr. Erdoğan ÖZBAY
December 2011, 73 pages

In this thesis, parameters of Engineered Cementitious Composites (ECC) design, which most possibly affecting the fresh, rheological and mechanical properties are investigated. An experimental program that contains thirty-six different mixtures was undertaken to evaluate the combined effect of following factors: water-binder (W/B), sand-binder (S/B), superplasticizer-binder (SP/B) ratios and maximum aggregate size (D_{max}) for the purpose of more effectively realizing mechanical properties optimized through micromechanical design theory. Mini-slump, Marsh cone, rotational viscometer were used to evaluate fresh and rheological properties of ECC. Compressive strength and four-point bending tests were used for mechanical characteristics on the 28 days age ECC specimens. Test results indicate that W/B, S/B and SP/B parameters strongly affect the fresh, rheological and mechanical properties while D_{max} only statistically effective on the mid-span beam deflection values of the ECC. The effects of studied parameter (W/B, S/B, SP/B and D_{max}) were characterized and analyzed using regression models, which can identify the primary factors and their interactions on the measured properties. Statistically significant regression models were developed for mini slump, Marsh cone, yield stress, plastic viscosity, compressive strength, mid-span beam deflection, modulus of rupture as function of W/B, S/B, SP/B and D_{max}. To find out the best possible ECC mixtue under the condition of this research concept for the desired workability and mechanical characteristics, a multi-objective optimization problem was defined and solved based on developed regression models.

Keywords: Engineered cementitious composites; rheology; factorial experimental design; optimization

ÖZET

UÇUCU KÜL İÇEREN TASARLANMIŞ ÇİMENTO BAĞLAYICILI KOMPOZİTLERİN REOLOJİK ÖZELLİKLERİ

BİLİCİ, Zafer
Yüksek Lisans Tezi, İnşaat Mühendisliği Bölümü
Tez Yöneticisi: Doç. Dr. Mustafa ŞAHMARAN
Yardımcı Tez Yöneticisi: Yard. Doç. Dr. Erdoğan ÖZBAY
Aralık 2011, 73 sayfa

Bu araştırmada, tasarlanmış çimento bağlayıcılı kompozitlerin (ECC) taze, reolojik ve mekanik özelliklerini etkileme ihtimali olan parametreler incelenmiştir. Mikromekanik tasarım yönetemleri ile opimizasyonu gerçekleştirilmiş olan ECC'nin mekanik özelliklerinin daha verimli bir biçimde belirlenebilmesi için su/bağlayıcı oranı (S/B), kum/bağlayıcı oranı (K/B), süperakışkanlaştırıcı/bağlayıcı oranı (SA/B) ve en büyük agrega tane boyutu (D_{mak}) parametrelerinin toplu etkilerinin araştırılması amacı ile 36 farklı ECC karışımı hazırlanmıştır. Mini-yayılma testi, Marsh hunisi ve rotasyonel viskozimetre deneyleri ile ECC karışımlarının taze ve reolojik özellikleri belirlenmiştir. Basınç dayanımı ve dört noktada eğilmede çekme dayanımı deneyleri 28 günlük sertleşmiş ECC numunelerinin mekanik özelliklerini belirlemek için kullanıldı. Deney sonuçları; S/B, K/B ve SA/B parametrelerinin ECC karışımlarının taze reolojik ve mekanik özelliklerini önemli ölçüde etkilerken, D_{mak} parametresi sadece ECC karışımlarının kiriş orta açıklık sehim kapasitesinin belirlenmesinde istatistiksel olarak etkili olduğunu göstermiştir. Mini yayılma testi, Marsh hunisi akma zamanı, rotasyonel viskozimetre, basınç dayanımı ve dört noktada eğilmede çekme dayanımları için test edilen parametrelerin istatistiksel olarak anlamlı regrasyon modelleri kuruldu. Bu şartlar altındaki en uygun işlenebilirlik ve mekanik özelliklerine sahip ECC karışımının tespit edilmesi için çok amaçlı optimizasyon problemi belirlenip çözümü gerçekleştirilmiştir.

Anahtar Kelimeler: Tasarlanmış Çimento Esaslı Kompozit (ECC), reoloji, faktöryel deneysel tasarım, optimizasyon

ACKNOWLEDGEMENT

Thanks to the Assoc. Prof. Dr. Mustafa ŞAHMARAN for teaching me this project with patience. Without his support, inspiration, dedication of time and energy throughout the past year, I could have never completed this work. I owe forever my sincerest gratitude to him, for opening my eyes to the innovative material technology world, and for challenging me with novel research ideas capable of solving real-world problems.

I must acknowledge the financial assistance of the Scientific and Technical Council of Turkey (TÜBİTAK) provided under Project: MAG-108M495.

My deep appreciations and thanks to Asst. Prof. Dr. Erdoğan ÖZBAY and Research Asistant Hasan Erhan YÜCEL for his helps and valuable suggestions.

I would also like to special thanks to Assoc Prof. Dr. Aytaç GÜVEN and Assist. Prof. Dr. Hüsnü UĞUR for serving on the thesis committee.

Finally, I would also thanks to my family for their support and encouragement during my study.

CONTENTS

LIST OF FIGURES

LIST OF TABLES

Page

LIST OF SYMBOLS/ABBREVIATIONS

μ	coefficient of viscosity
ASTM	American society for testing and materials. West Conshohocken
C	Cement
δ_0	corresponding crack opening
d_f	fiber diameter
D_{max}	maximum aggregate size
ECC	Engineered Cementitious Composites
$e^{f\phi}$	accounts for the changes in bridging force for fibers crossing at an inclined angle to the crack plane
E_m	elastic modulus of the mortar matrix
ϕ	orientation angle of the fiber
FA	class f fly ash
FA/C	fly ash to cement ratio
HPFRCC	High performance fiber reinforced cementitious composites
J'_b	complimentary energy
JCI	Japan Concrete Institute
J_{tip}	fracture energy of the mortar matrix
K_m	fracture toughness of the mortar matrix
MSFRCC	Mechanical behaviours of a multi-scale fiber reinforced cement composite
$P(\delta)$	pullout load versus displacement relation of a single fiber aligned normal to the crack plane
$p(\phi))$	probability density functions of the fiber orientation angle
p(z)	centroidal distance from the crack plane, respectively
PE	polyethylene
PVA	poly-vinyl-alcohol fiber
RH	reletive humidity
S/B	sand to binder ratio
σ_0	maximum crack bridging stress
SCC	self compacted concrete
sfc	maximum crack bridging stress
SP/B	Superplasticizer to binder ratio

V_f	fiber volume fraction
W/B	Water to binder ratio
τ_0	yield stress
SP	Superplasticizer
T	torque
N	rotational speeds
LVDT	Linear variable displacement transducer
SEM	scanning electron microscopy
MIP	mercury intrusion porosimetry
ANOVA	analysis of variance
ρ	degree of contribution
a_i	the model constants
E	random error term
d_j	desirability functions

CHAPTER I

INTRODUCTION

General Information

Engineered Cementitious Composites (ECC) is a special type of high performance fiber-reinforced cementitious composite featuring high ductility and damage tolerance under mechanical loading, including tensile and shear loadings [Li, 1997; Li, 2003; Li, 2001]. By employing micromechanics-based material optimization [Li, 1997; Lin, 1997], tensile strain capacity in excess of 3% under uniaxial tensile loading can be attained with only 2% fiber content by volume [Li, 1997 ; Lin, 1999]. Figure 1.1 shows a typical uniaxial tensile stress-strain curve of an ECC containing 2 vol. % of poly-vinyl-alcohol fiber (PVA fiber). The characteristic strain-hardening after matrix first cracking is accompanied by sequential development of multiple microcrackings and the tensile strain capacity is 300-500 times greater than that of normal concrete. The crack width development during inelastic straining is also shown in Figure 1.1. Even at ultimate load, the crack width remains on the order of 50 to 80 micrometer. This tight crack width is self-controlled and, whether the composite is used in combination with conventional reinforcement or not, it is a material characteristic independent of rebar reinforcement ratio. In contrast, normal concrete and fiber-reinforced concrete rely on steel reinforcement for crack width control. The tight crack width of ECC is important to the durability of ECC structures as the tensile ductility is to the structural safety at ultimate limit state.

These properties, together with a relative ease of production including self-consolidation casting [Kong, 2003 a; Kong, 2003b] and shotcreting [Kim, 2003], make them suitable for various civil engineering applications. ECC is currently emerging in full scale structural applications [Kunieda, 2006; Li, 2005].

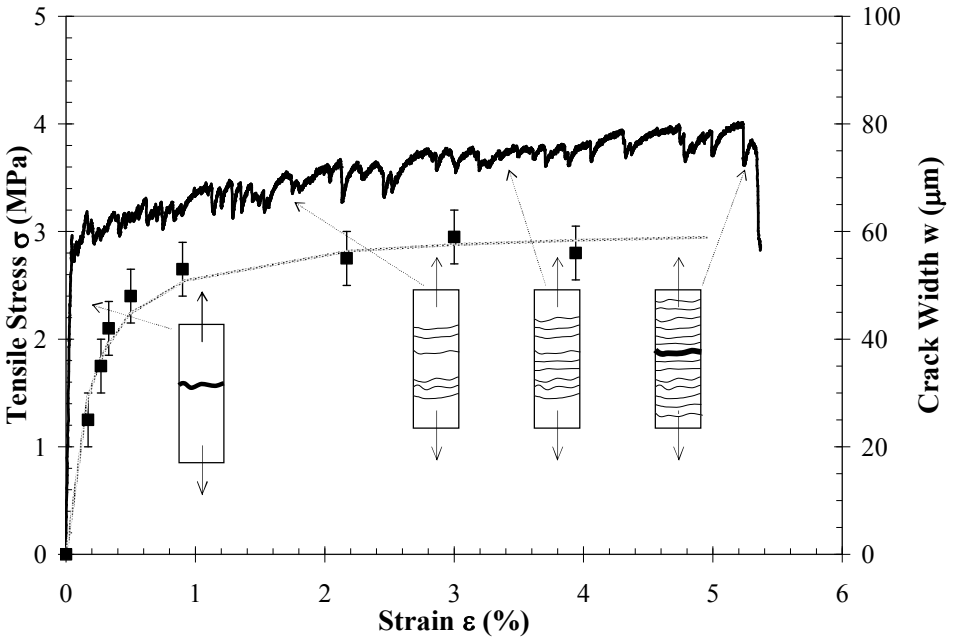

Figure 1.1 Typical tensile stress-strain curve and crack width development of PVA-ECC

ECC is designed by considering the criteria of micromechanical design theory, which is a technique to tailor the microstructure of the composite based on the understanding of the mechanical interactions between the matrix, fiber, and interface phases under mechanical loading. In order to obtain desired high ductility, fiber must be well dispersed in the ECC matrix, however, in some cases, because of the lack of perfect fiber dispersion or inhomogeneous distribution of fibers, ECC tends to degrade as well as introduce undesirable variability into the mechanical properties. Moreover, ingredients with inappropriate characteristics (type, size, and amount) as defined by micromechanical principles and ingredients from different sources and/or processing procedures lead to a change in fresh and hardened properties of ECC. In this scenario, material ingredient retailoring has to be applied through ECC material design theory in order to regain high tensile ductility [Wang, 2006]. For this purpose, in-depth knowledge of micromechanics and microstructural design theory is invaluable. It is believed that composite microstructure that governs ECC material properties are strongly influenced by processing details [Li, 2006], as depicted in Figure 1.2. As example, processing may affect fiber dispersion uniformity and defect size distribution which have direct bearings on composite properties. Therefore, the second reason maybe that ingredients from different sources lead to a change in

rheological properties of fresh ECC even when applying the same mix design, which in turn impacts negatively on hardened properties. It is suggested in this thesis that the rheological control of fresh properties in producing ECC needs to be clearly defined in order to realized optimum hardened properties predicted by micromechanics.

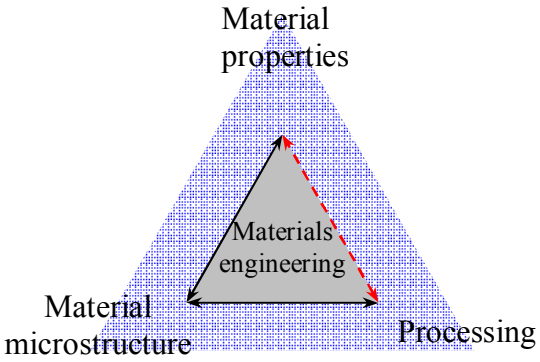

Figure 1.2 ECC material properties as a function of material microstructure influenced by processing

1.2 Research Objectives and Scope

This thesis focuses on the effect of main ECC design parameters such as water-binder ratio (W/B), sand/binder ratio (S/B), superplasticizer/binder ratio (SP/B) and maximum aggregate size (D_{max}) on the fresh, rheological and mechanical properties of ECC and trying to find out the optimal ECC mixture design for the performance maximization. For this purpose, a factorial experimental design program was performed by considering the W/B, S/B, SP/B and D_{max} parameters to carry out their effectiveness on realizing the desired fresh (mini-slump flow diamter and Marsh cone flow time), rheological (yield stress and plastic viscosity) and mechanical (number of crack and crack size, mid-span beam deflection, flexural and compressive strengths) properties. Then, the influences of each parameter and their interactions were characterized and analyzed statistically. After that, regression models were developed for mini slump flow diameter, Marsh cone flow time, yield stress, plastic viscosity, compressive strength, mid-span beam deflection capacity, modulus of rupture as function of W/B, S/B, SP/B and D_{max}. Finally, for the desired workability and mechanical characteristics, best possible ECC mix under the constraints of this

research was defined by satisfying the mutual objectives. This thesis is organized according to the investigation framework depicted in Figure 1.3

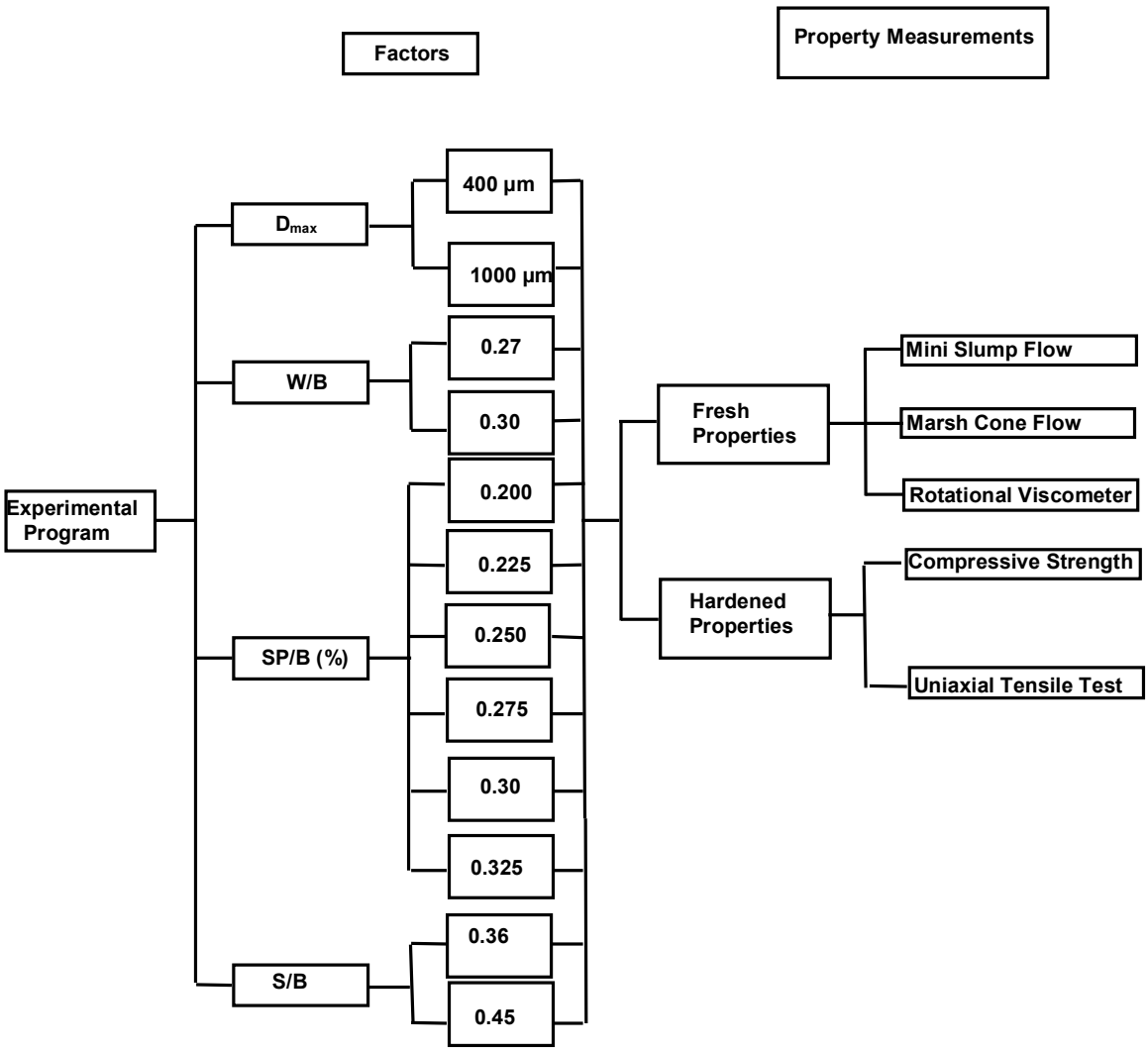

Figure 1.3 Flowchart for experimental program

In Chapter 2, properties of ECC, and rheological properties of cementitious composites are discussed. In Chapter 3, the materials used in ECC production and experimental programs are discussed. The results of the experimental studies are presented and discussed in Chapter 4. The conclusions of the research are presented in Chapter 5.

CHAPTER II

LITERATURE REVIEW AND BACKROUND

2.1 Introduction

Around the globe, nations struggle with ever increasing challenges of development. The consequences of this struggle are often most visible in developing nations with rapidly expanding economies. Often, the backbone of such rapidly expanding economies is infrastructure development in the form of highways, bridges, dams, airports, marine structures and buildings, which support trade and encourage outside investment. Therefore, concrete material is, literally, one of the building blocks of economic development.

While essential for the development of economies, the construction and maintenance of these infrastructures often requires large volumes of portland cement and aggregate for use in concrete structures. The production of these materials can result in tremendous public health impacts decades into the future. To illustrate, the production of one ton of Portland cement releases 6.3 mg of particles less than 10 microns in diameter (PM_{10}) into the atmosphere. Numerous deaths annually have been attributed to atmospheric PM_{10} concentrations as low as 20 mg/m^3. In addition to direct public health concerns, the production of portland cement requires 4 GJ of energy per tonne, and releases into the atmosphere approximately 1 tonne CO_2 per tonne of cement, representing in total 7% of worldwide CO_2 emissions, and significantly contributing to global warming due to ozone depletion. Furthermore, mining large quantities of raw materials such as limestone and clay, and fuel such as coal, often results in extensive deforestation and top-soil loss. As a case study, the country of Turkey has seen cement production increase from 30 million tonnes in

year 2001 to more than 70 million tonnes in 2010 (Source: Turkish Cement Manufacturers Association). Due to this rise in production, capacity utilization with Turkey has increased from 46% to over 80% from 2001 to 2010 requiring construction of new cement plants in the near future if demand does not fall. Moreover, as in the cement production, mining of the aggregates used in concrete production causes significant ecological damage. The overall consequence is an inherent unsustainable system measured by economic, environmental, and social indicators. Sustainability requires the application of energy efficient materials with low impact on environment and improved durability. Therefore, the production of concrete is a serious concern for global environmental sustainability. In spite of these environmental problems, the global demand for concrete increases at a very rapid pace, largely driven by the construction boom in developing countries; and in less than one century, concrete has become the most widely used construction material in the world. Concrete is now used not only for buildings but also for highways, bridges, underground mass transit facilities, wastewater treatment systems, and marine structures.

In European Design Codes, a service life time of 75+ for concrete structures are now required from large public works. But experience has shown that under the combined effects of mechanical loads and environments, many infrastructures begin to deteriorate after only 20 or 30 years. The short service life of Portland cement concrete infrastructures has significant impacts due to materials production for repair and replacement of deteriorated infrastructure, along with fuel consumption and vehicle emissions from construction related traffic congestion. The poor durability of reinforced portland cement concrete infrastructure associated with concrete cracking is one of the main reasons for this short service life of concrete infrastructure. Cracking is usually a result of various physical, chemical, and mechanical interactions between concrete and its environment, and it may occur at different stages throughout the life of a structure. The formation of cracks coupled with a lack of crack width control in brittle concrete are primarily responsible for two damaging phenomena; reduce the strength and stiffness of the concrete structure, and accelerate the ingress of aggressive ions, leading to other types of concrete deterioration such as corrosion, alkali-silica reaction, and sulfate attack, and resulting in further cracking

and disintegration. Therefore, durability is vitally important for all concrete structures, and it can be associated with the brittle nature of concrete.

2.1.1 Engineered Cementitious Composites (ECC)

During the last decade concrete technology has been undergoing rapid development. The effort to modify the brittle behavior of plain cement materials such as cement pastes, mortars and concretes has resulted in modern concepts of high performance fiber reinforced cementitious composites (HPFRCC) that exhibit pseudo-ductile behavior under tension load. In plain concrete, after the crack there is no load carrying capacity. In conventional fiber reinforced cementitious composites, matrix cracking is followed by a reduction in load carrying capacity known as residual strength (lower curve in Figure 2.1). For HPFRCC, after the formation of the first through crack, the fibers themselves are able to carry additional load. On further loading, multiple micro cracks will form along the member, leading to a significant increase in strain. The tensile stress-strain curve will hence exhibit a post-cracking hardening branch similar to that of ductile materials (upper curves in Figure 2.1). The quantitative criterion for the achievement of pseudo-ductility (inelastic straining), in terms of various material and geometric parameters (such as properties of fiber, matrix (composite without fiber) and interface, fiber length and volume fraction, etc.), was proposed by Li and Leung [Li and Leung, 1992] and further developed by Li [Li, 1993], and Kanda and Li [Kanda, 2003; Li, 1999]. With proper selection of parameters to fulfill the criterion, pseudo-ductile composites with different strengths can be made with fiber volume from 1.5% to 5%. The actual 'ductility' of the HPFRCC, which can be defined as the strain at maximum tensile stress, depends on the effectiveness of fibers in transferring stress back into the matrix (which in turn depends on the micro parameters) as well as the toughness of the matrix itself. Normally, the higher the matrix toughness, the lower will be the ductility achieved with a certain fiber volume fraction. Depending on the particular application, the material design can be varied to produce an optimal tensile stress vs. strain relation that satisfies the strength and ductility requirements. In the literature, HPFRCC's have been given different names by various researchers. These include MSFRCC [Rossi and Parant, 2005], CARDIFRC [Alaee and Karihaloo, 2003] and hybrid fiber composites [Markovic, 2004], which are the high strength composites with relatively

low ductility, as well as ECC [Li, 1993], a highly ductile HPFRCC with moderate fiber volume (tensile failure occurs at 2-5% strain – 200-500 times that of conventional concrete or fiber reinforced concrete) with relatively low strength. The high ductility of ECC is achieved by multiple cracking with crack width self-limited to about less than 100 μm.

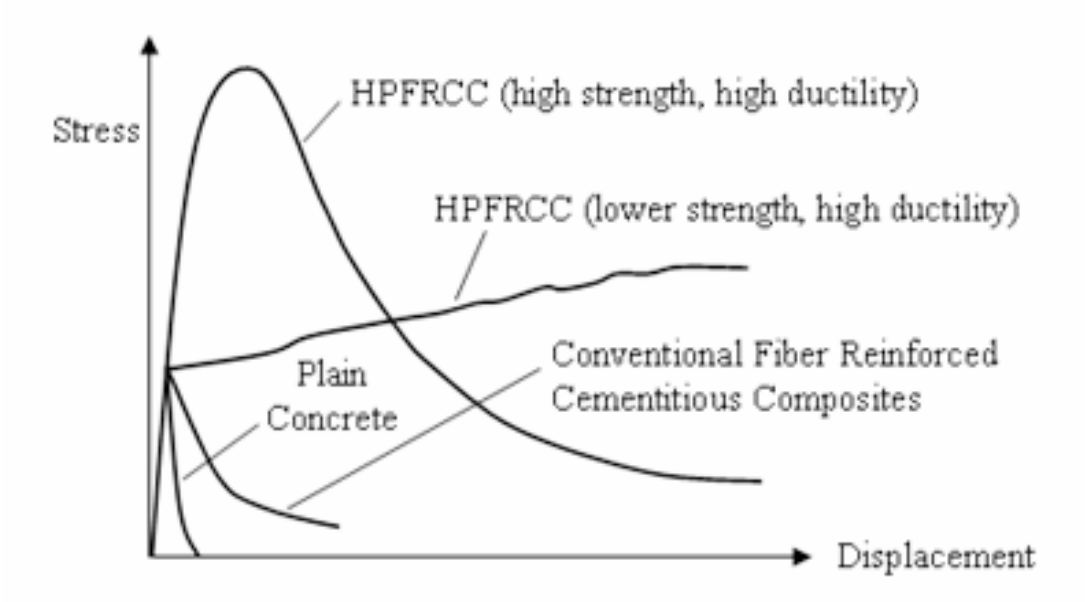

Figure 2.1 Tensile behavior of plain and fiber reinforced cementitious materials

ECC promises to be used in a wide variety of civil engineering applications, as summarized in Japan Concrete Institute [JCI, 2002] and by [Kunieda and Rokugo, 2006]. One of the most promising areas of application of this material is in the repair of concrete structures. Several investigations on the advantages of structures repaired by ECC have been carried out. Lim and Li [Lim and Li, 1997] found the mechanical advantages of an interface crack trapping mechanism within ECC/reinforced concrete composites. Li and Li [Li and Li, 2009]demonstrated that to suppress both repair surface cracking and repair/old interface delamination, the repair material needs to exhibit "inelastic straining – tensile ductility" to accommodate its shrinkage deformation, thus relieving the stresses built-up under restrained drying shrinkage conditions. By this means, surface crack width and interface delamination can be both minimized. Inelastic straining in the form of micro-crack damage has been demonstrated in ECC. Moreover, the self-healing of cracks becomes prominent when crack width is small. If durability, and eventually sustainability are important goals,

current construction practice and the codes of recommended practice must undergo a paradigm shift to achieve concrete structures that have tight cracks or are "crack-free" in preference to high strength. The formation of cracks coupled with a lack of crack width control in brittle concrete are primarily responsible for two damaging phenomena; reduce the strength and stiffness of the concrete structure, and accelerate the ingress of aggressive ions, leading to other types of concrete deterioration such as corrosion, alkali-silica reaction, and sulfate attack, and resulting in further cracking and disintegration. As a result, these cracks can dramatically reduce the long-term durability performance of concrete. While it is unrealistic to imagine the complete suppression of cracking in concrete, the ability to use robust self-healing functionality as an autogenous mechanism in areas with tight cracks may lead to the realization of such virtually "crack free" concrete. In 2002, the Concrete Research and Education Foundation also listed such robust self-healing concretes second in its list of "high priority research topics" for the concrete industryi. Self-healing is generally attributed to the hydration of previously unhydrated cementitious material, calcite formation and expansion of the concrete in the crack flanks, crystallization, closing of cracks by solid matter in the water and closing of the cracks by spalling of loose concrete particles resulting from cracking. Self-healing of cracks should be taken into account when specifying tolerable crack widths. Evardsen, and Reinhardt and Joss proposed that cracks of less than 100 μm can easily be closed by self healing process.

The ductile behavior and self-healing characteristic of ECC is associated with many other desirable properties for repair and rehabilitation applications. These include (i) high energy absorption, impact resistance and tensile ductility (high inelastic strain), (ii) ability to redistribute localized stresses, thus reducing the sensitivity of the material to stress concentrations, (iii) high deformability, passing ability, and resistance to segregation to secure complete filling of complex formwork and ease of production including self-consolidation casting and shotcreting (iv) high shear strength, (v) high bond strength to steel reinforcement and substrate concrete (high delamination resistance), and (vi) capability to control the opening of cracks, and hence preventing the resulting increase of transport properties that would lead to durability problems. However, three major limitations of ECC are the high cost, environmental issues and high shrinkage of the material. The cost is high because

fibers are much more expensive than the basic components of conventional concrete. Currently, poly-vinyl alcohol (PVA), polyethylene (PE), and micro-steel fibers are only successfully used in the production of ECC. Compared with conventional concrete, ECC materials contain considerably higher cement content, typically two to three times higher. Table 2.1 shows the mixture proportions of typical PE-ECC and PVA-ECC along with conventional structural concrete. The high cement content in ECCs is a consequence of rheology control for easy fiber dispersion and, more essentially, matrix toughness control for strain-hardening behavior. To achieve high ductility (strain-hardening), matrix fracture toughness has to be limited such that multiple cracking could occur before reaching maximum fiber bridging stress. Large aggregates are hence eliminated in the mixture, resulting in a higher cement content compared with normal concrete. In fact, ECC materials use cement paste or mortar with fine sand as a matrix, and typically have cement content at 800 to 1200 kg/m3. High cement usage results in undesired high hydration heat as well as high material cost. In addition, such matrices apparently compromise sustainability performance of the material, as cement production is responsible for 6% of global greenhouse gas emissions generated by human activities, and significant levels of nitrogen oxides, particulate matter, and other pollutants. Moreover, ECC could generate relatively large shrinkage strain compared to conventional concrete due to relatively high cement content, low water-cement ratio and lack of coarse aggregate, thus increasing cracking potential of the concrete. However, the presence of fibers can control the crack width such that deterioration is not an issue.

Table 2.1: Typical mixture proportions of concrete and ECCs

Material (kg/m^3)	**PVA ECC**	**PE-ECC**	**Conventional Concrete**
Portland Cement	*832*	1205	390
Water	366	314	166
Fly ash	-	-	-
Aggregates	832	603	1717
Fiber	26	17	-
Superplasticizer	17	12	2

2.1.2 Design of Engineered Cementitious Composites

The first priority when designing ECC material is to ensure the formation of multiple cracks and strain-hardening behavior under load. This allows large deformations to be distributed over multiple micro-cracks. The basis of multiple micro-cracking and strain hardening within ECC is the propagation of steady state cracks which were first characterized by Marshall and Cox [Marshall and Cox, 1988], and extended to fiber reinforced cementitious composites by Li and Leung [Li and Leung, 1992] and Lin et al. [Lin, 1999]. By forming steady state "flat cracks" which maintain a constant crack width while propagating, rather than Griffith-type cracks which widen during propagation as in typical tension-softening fiber reinforced cementitious materials, ECC material exhibits multiple micro-cracks which saturate the specimen while undergoing strain-hardening during extreme tensile deformation. The formation of multiple steady state cracking is governed by the bridging stress versus crack width opening relation along with the cracking toughness of the mortar matrix. To achieve this phenomenon the inequality shown in Equation-2.1 must be satisfied.

$$J_b^{'} = \sigma_0 \delta_0 - \int_0^{\delta_0} \sigma(\delta) d\delta \geq J_{tip} \approx \frac{K_m^2}{E_m} \tag{2.1}$$

where J'_b is the complimentary energy shown in Figure 2.2, σ_0 and δ_0 are the maximum crack bridging stress and corresponding crack opening, J_{tip} is the fracture energy of the mortar matrix, K_m is the fracture toughness of the mortar matrix, and E_m is the elastic modulus of the mortar matrix. In addition to the fracture energy criterion, a strength criterion expressed in Equation-2.2 must be satisfied.

$$\sigma_0 > \sigma_{fc} \tag{2.2}$$

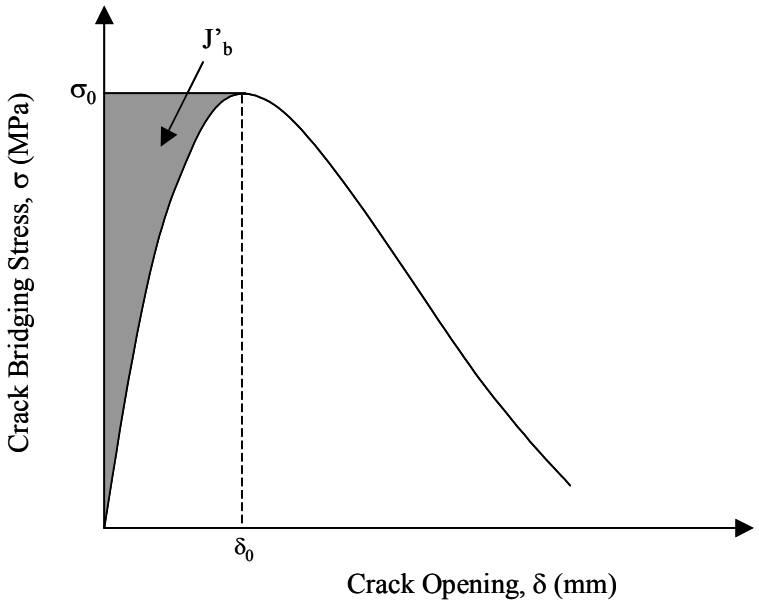

Figure 2.2 Crack bridging stress versus crack opening relation

where, σ_0 is the maximum crack bridging stress and σ_{fc} is the first cracking strength of the mortar matrix. For saturated multiple cracking, Wang and Li [Wang and Li, 2004] found that Equation-2.2 must be satisfied at each potential crack plane, where σ_{fc} is understood as the cracking stress on that crack plane.

Once an ECC mixture is selected which sufficiently meets the two above criteria, the formation of multiple steady state cracks, and strain-hardening performance, can be realized. However, in addition to forming these cracks, the material must also be designed to exhibit crack widths below the 100 μm threshold limit. This can be achieved through tailoring of the crack bridging versus crack opening relation referenced in Equation-2.1. The maximum steady state crack width exhibited during ECC multiple cracking can be assumed to be δ_0, the crack width corresponding to the maximum crack bridging stress, σ_0, as shown in Figure 2.2. If the crack width were to grow beyond δ_0, the crack bridging stress would begin to fall, in which case the crack would localize and multiple crack formation would cease. By keeping δ_0 below the 100 μm threshold, the ECC material can exhibit multiple cracking and strain hardening performance.

Lin et al. [Lin, 1999] proposed the formulation of the crack bridging stress versus opening relationship based on summing the bridging force contribution of fibers that cross a given crack plane. This relation in expressed in Equation-2.3.

$$\sigma(\delta) = \frac{4V_f}{\pi d_f^2} \int_{\phi=0}^{\pi/2} \left(\int_{z=0}^{(L_f/2)\cos\phi} P(\delta) e^{f\phi} p(\phi) p(z) dz \right) d\phi \qquad (2.3)$$

where V_f is the fiber volume fraction, d_f is the fiber diameter, ϕ is the orientation angle of the fiber, L_f is the fiber length, z is the centroidal distance of a fiber from the crack plane, f is a snubbing coefficient, and $p(\phi)$) and p(z) are probability density functions of the fiber orientation angle and centroidal distance from the crack plane, respectively. $P(\delta)$ is the pullout load versus displacement relation of a single fiber aligned normal to the crack plane, also described in Lin et al. [Lin, 1999]. The factor $e^{f\phi}$ accounts for the changes in bridging force for fibers crossing at an inclined angle to the crack plane.

Using these basic micromechanical models to tailor the ECC material, a composite can be designed to undergo large deformations, up to several percent, without sacrificing low permeability due to large crack widths. The application of material design procedures, such as those outlined above, allow materials engineers to carefully match material characteristics to specific structural demands, such as strain capacity and low permeability.

2.2 Rheology of Cementitious Composites

Characteristic phenomena of liquid and gas to immediately deform when subjected to small shearing stresses is called “flow”. The study of flow process that deals with relations between stress, strain and their time dependent derivative is called “rheology” [Ozawa and Maekawa, 1989]. In practice, rheology is concerned with materials whose flow properties are more complicated than those of a simple fluid (liquid or gas) or an ideal elastic solid [Tattersall and Banfill, 1983]. The rheological (flow) properties of concrete are important for the construction industry because concrete is usually put into place in its plastic form [Ferraris, 1999].

Concrete and mortar are composite materials, with aggregates, cement, and water as the main components. Concrete is a concentrated suspension of solid particles (aggregates) in a viscous liquid (cement paste). Cement paste is not a homogeneous fluid and is itself composed of particles (cement grains) in a liquid (water).

Normally there are two types of flow behavior: Newtonian fluid and non-Newtonian fluid. For a Newtonian fluid, the shear stress divided by the rate of shear is constant and called the coefficient of viscosity (μ) which is used as a physical characteristic of the material (Figure 2.3). In the non-Newtonian fluid, when the shear rate is varied, the shear stress does not vary in the same proportion and same direction. The viscosity of non-Newtonian fluid changes as the shear rate varies [Ferraris, 1999].

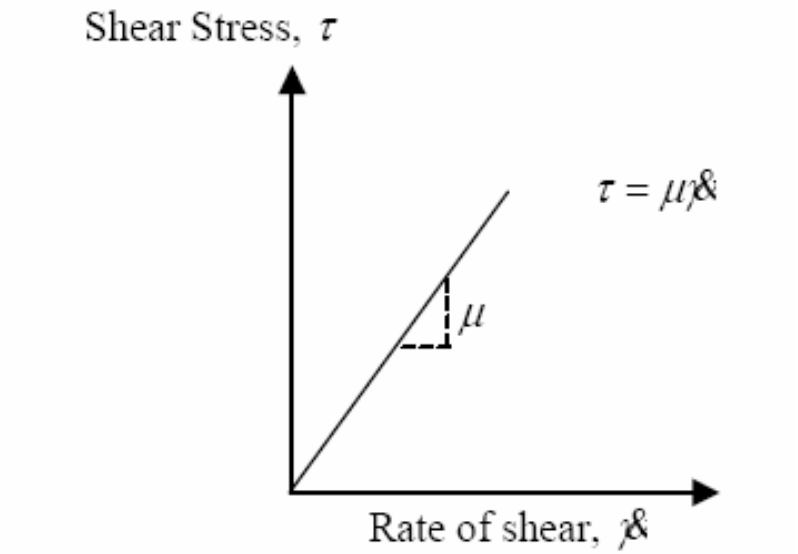

Figure 2.3 Newtonian fluid

Paste, mortar, and concrete are considered as non-Newtonian fluid. The rheology of fresh concrete is most often described by the Bingham model (Figure 2.4). In this model the flow curve has an intercept on the stress axis, indicating a minimum stress which is required to start the flow [Tattersall and Banfill, 1983]. According to this model, fresh concrete must overcome a limiting stress (yield stress, τ_0) before it can flow. Once the concrete starts to flow, shear stress increases linearly with an increase in strain rate as defined by plastic viscosity. The plastic viscosity is the measure of how easily the material will flow, once the yield stress is overcome. Therefore, in order to fully describe the rheological properties of fresh concrete by Bingham model

two parameters, namely the plastic viscosity and the yield stress are necessary [Ozawa and Maekawa, 1989].

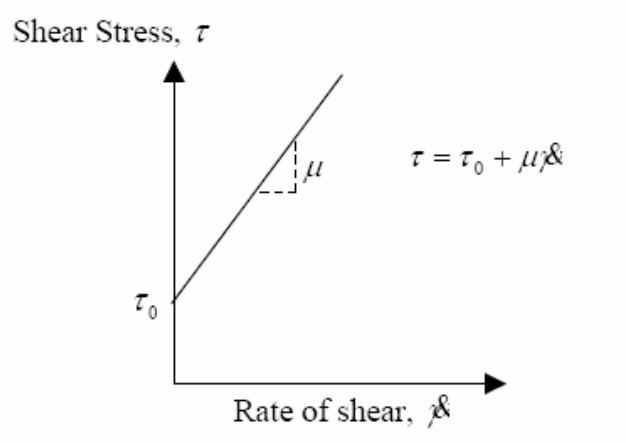

Figure 2.4 Bingham model for fluid

The lower yield stress gives less resistance to start the flow of concrete. Higher viscosity prevents segregation but provides high resistance to the flow of concrete. It is important for self compacted concrete (SCC) to have low yield stress and moderate viscosity to ensure enough flow and to prevent segregation [Saak, 2001; Lacombe, 1999]. Most of the widely used tests are unsatisfactory in that they measure only one parameter, which does not fully characterize the concrete rheology. Figure 2.5 shows how two concretes could have one identical parameter and a very different second parameter. These concretes may be very different in their flow behaviors. Therefore, it is important to use a test that will describe the concrete flow, by measuring (at least) both factors [Ferraris, 1999].

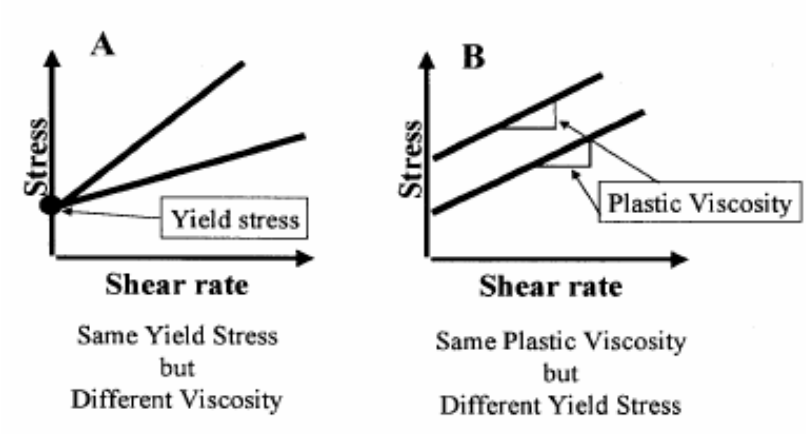

Figure 2.5 Concrete rheology [Ferraris, 1999]

The rheological properties of fresh concrete are determined by the so-called rheometers, which measure the shear stress at varying shear rates. Unfortunately the inherent properties of concrete make it impossible to use the rheometers designed for neat fluids without any solid particles. Therefore, there isn't a consensus on the rheological properties of SCC that are available in the market [NIST, 1999]. In a comprehensive study by NIST, a series of twelve concrete mixtures was tested by five rheometers. The mixtures had slumps ranging from 90 mm to 235 mm, but more importantly, they had a wide range of combinations of yield stress and plastic viscosity. It was found that the rheometers gave different values of the Bingham constants of yield stress and plastic viscosity, even for those instruments that give these directly in fundamental units [NIST, 1999].

CHAPTER III

EXPERIMENTAL PROGRAM

3.1 Material Parameters Constrained by Micromechanics and Unconstrained Parameters Governing Fresh Properties

The ingredients and mix proportions of ECC are optimized through micromechanics-based material design theory to satisfy strength and energy criteria to attaining high composite tensile ductility [Li, 1997; Li, 2003; Li, 2001; Yang, 2006]. The type, size and amount of fiber, matrix ingredients and interface characteristics are tailored for multiple cracking and controlled crack width in ECCs. Specifically, high aggregate content and presence of coarse aggregates lead to a tough matrix which delays crack initiation and prevents steady-state flat-crack propagation in ECC, resulting in loss of tensile ductility. Therefore, instead of coarse aggregate, ECC incorporates fine silica sand with sand to binder ratio (S/B) of 0.37 to maintain adequate stiffness and volume stability [Li, 1995]. The binder system is defined as the total amount of cementitious material, i.e. cement and fly ash in ECC. The silica sand has a maximum grain size of 250 μm and a mean size of 110 μm. Another purpose of using fine silica sand is to obtain the optimum gradation of particles to produce good workability [Fischer, 2003].

Fly ash has been used to replace cement in ECC mix design for a number of reasons. The absence of coarse aggregate in ECC results in a higher cement content. Partial replacement using fly ash reduces the environmental burden. Further, it has been found that incorporating high amount of fly ash, especially Class-F fly ash, can reduce the matrix toughness and improve the robustness of ECC in terms of tensile ductility. Additionally, unhydrated fly ash particles with small particle size and

smooth spherical shape serve as filler particles resulting in higher compactness of the fiber/matrix interface transition zone that leads to a higher frictional bonding. This aids in reducing the steady-state crack width beneficial for long-term durability [Lepech, 2005a; Lepech, 2005b] of the structure. However, excessive fly ash decreases the compressive strength of ECC. In this experimental study, a high fly ash to cement ratio (FA/C) of 2.2 was chosen to satisfy the above requirements, while still maintaining adequate compressive strength similar to that of normal strength concrete.

Although various fiber types have been used in the production of ECC, PVA fiber was adopted in the current version of ECC. The use of PVA fiber was decided based on the composite performance and economics consideration and PVA-ECC represents the most practical ECC used in the field [Kunieda, 2006; Li, 2005] at the present. The dimensions of the PVA fiber are 8 mm in length and 39 μm in diameter. The nominal tensile strength of the fiber is 1600 MPa and the density of the fiber is 1300 kg/m^3. The PVA fiber is surface-coated by hydrophobic oil (1.2% by weight) in order to reduce the fiber/matrix interfacial bond strength. To account for material inhomogeneity, a fiber content of 2% by volume in excess of the calculated critical fiber content has been typically used in the mix design. These decisions were made through ECC micromechanics material design theory and had been experimentally demonstrated to produce good ECC properties in previous investigations [Li, 2001; Kong, 2003; Li, 2001].

From the above discussion, FA/C, and fiber type, dimension, and content may be considered as constraints in this study. They are treated as fixed parameters in the present study. Their specific details, summarized above, should lead to optimal composite properties, according to micromechanics. However, improper processing may lead to non-uniform fiber dispersion, inappropriate flaw size and distribution, or other microstructures not conducive to multiple cracking. Suitable processing control is necessary to realize composite materials with expected optimal properties.

In this study, effect of four parameters, which are water-binder ratio (W/B), sand/binder ratio (S/B), superplasticizer/binder ratio (SP/B) and maximum aggregate size (D_{max}), were studied by committed to the micromechanical design. All of these

parameters were constrained in ECC mix design so the ranges of studied parameters for factorial experimental design were kept in narrow interval. It was aimed to find out effect of some fine tuning on the important design parameters governing the fresh, rheological and mechanical properties of ECC in the present study:

- W/B ratio (by mass), often used to adjust the workability of cementitious materials and it was studied as 0.27 (ratio standard ECC M45 design) and 0.30;

- S/B (by mass), defined as the ratio of the amount of sand to total binder (Portland cement + fly ash), is used to find out the effect of sand content increment and it was studied as 0.36 (ratio standard ECC M45 design) and 0.45;

- SP/B (%), reflecting the amount of superplasticizer (SP), a commonly used admixture to enhance the fluidity of cementitious materials; and studied as the percent of (0.200%, 0.225%, 0.250%, 0.275%, 0.300% and 0.325%) binder content

- D_{max}, is used to clarify the how the change of maximum aggregate size (D_{max}) will effect the properties of ECC. Two different sizes of D_{max} were studied, 400 μm and 1000 μm. In standard ECC (ECC M45) D_{max} was 200 μm.

These four factors are selected as "processing" variables in the following design of experiment (DOE) study.

3.2 Materials

3.2.1 Cement

The cement used in all mixtures was a normal portland cement CEM I 42.5R (C), which correspond to ASTM Type I cement. It had a specific gravity of 3.06 and Blaine fineness of 325 m^2/kg. Chemical composition and physical properties of cement are presented in Table 3.1.

The particle size distributions of cement, obtained by a laser scattering technique, is given in Figure 3.1

Table 3.1 Chemical properties of Portland cement and fly ash

Chemical composition	**Cement**	**Fly Ash**
CaO (%)	61.43	1.64
SiO_2 (%)	20.77	56.22
Al_2O_3 (%)	5.55	25.34
Fe_2O_3 (%)	3.35	7.65
MgO (%)	2.49	1.80
SO_3 (%)	2.49	0.32
K_2O (%)	0.77	1.88
Na_2O (%)	0.19	1.13
Loss of ignition (%)	2.20	2.10
$SiO_2+Al_2O_3+Fe_2O_3$	29.37	89.21
Physical properties		
Specific gravity	3.06	2.31
Blaine fineness (m^2/kg)	325	290

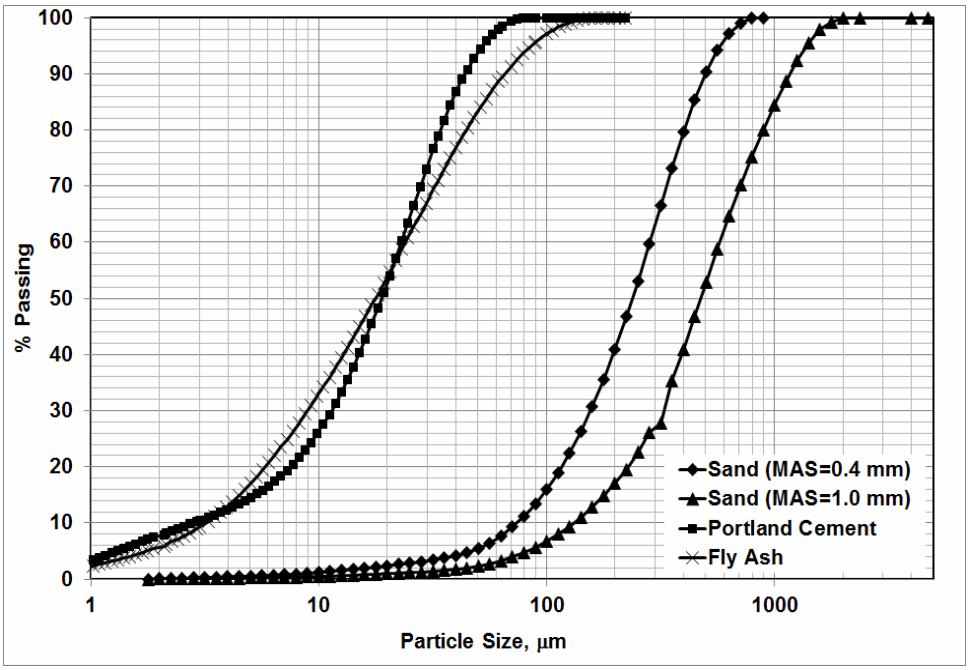

Figure 3.1 Particle size distributions of cement, fly ash, and aggregates

3.2.2 Fly Ash

Class-F fly ash (FA) conforming to ASTM C 618 (2003) requirements with a lime content of 1.64% obtained from Sugözü Thermal Power Plant was used. The chemical properties of FA are given in Table 3.1. The specific gravity and Blaine fineness of FA are 2.31 and 290 m^2/kg, respectively. The particle size distribution of FA is provided in Figure 3.1. Figure 3.2 illustrates the particle morphology of FA. The SEM image shows that both fly ashes have smooth spherical particles.

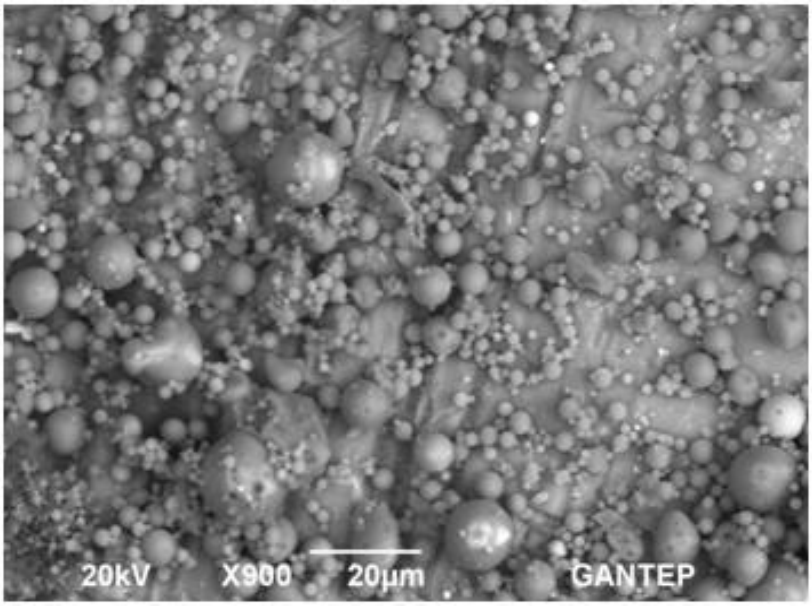

Figure 3.2 Particle morphology of fly ash determined by SEM

3.2.3 Aggregate

According to micromechanic-based design of ECC, exhibiting ductile and showing a large crack number, but small in width, a low toughness of the matrix is required. However, with the increase of maximum grain size of aggregate, increase in toughness of the matrix is appeared and as a result, to obtain suitable ECC, aggregate grain size is limited [Li, 1995]. Therefore, so far, ECC has been produced successfully with an average grain size of about 110 µm [Li, 1995]. Using high volumes of industrial by-product in the production of ECC decreases matrix toughness and provides freedom of changing aggregate size. It is very important to produce ECC from normal size local sources of aggregate in terms of widespread

application for both literature and our country. For this purpose, in the production of ECC, fine quartz with two maximum aggregate sizes (D_{max}) of 400 μm and 1000 μm was obtained from local sources in our country's resources. Water absorption capacity and specific weight of quartz aggregate used is 0.3% and 2.60, respectively. The grain size distribution curves for these aggregates are presented in Figure 3.1.

3.2.4 Chemical Admixtures

To improve the workability of ECC mixtures, Glenium 51, superplasticizer (SP – polycarboxylate ether as an active ingredient with 2.1 specific gravity and 40% solid content) produced by BASF Construction Chemicals was used.

3.2.5 Polyvinyl Alcohol (PVA) Fiber

Although various fiber types have been used in the production of ECC, PVA fiber was used in this study (Figure 3.3). The use of PVA fiber was decided based on and PVA-ECC represents the most practical ECC used in the field [Li, 2001; Kunieda and Rokugo, 2006] at the present. PVA fibers have attracted most attention due to the outstanding composite performance and economics consideration. The dimensions of the PVA fiber are 8 mm in length and 39 μm in diameter. The nominal tensile strength of the fiber is 1620 MPa and the density of the fiber is 1300 kg/m^3. The mechanical and geometric properties of PVA fibers are summarized in Table 3.2. The PVA fiber is surface-coated by hydrophobic oil (1.2% by weight) in order to reduce the fiber/matrix interfacial bond strength. To account for material inhomogeneity, a fiber content of 2% by volume in excess of the calculated critical fiber content has been typically used in the mix design. These decisions were made through ECC micromechanics material design theory and had been experimentally demonstrated to produce good ECC properties in previous investigations [Li, 2001; Kong, 2003].

Figure 3.3 PVA Fiber used in the production of ECC

Table 3.2 Mechanic and geometric properties of PVA fibers

Fiber Type	Nominal Strength (MPa)	Apparent Strength (MPa)	Diameter (μm)	Length (mm)	Young Modulus (GPa)	Strain (%)	Specific Weight kg/ m^3
PVA	1620	1092	39	8	42.8	6.0	1300

3.3 ECC Mixing and Specimen Preparation

The experimental program was based on a 2 (D_{max}) × 2 (water/binder) × 2 (sand/binder) × 6 (superplasticizer/binder). In total thirty-six mixtures with two different sand sizes (400 μm and 1000 μm), two water and binder ratio contents (0.27 and 0.30), two sand and binder ratio (0.36 and 0.45), and six superplasticizer to binder ratio (%0.200, 0.225, 0.250, 0.275, 0.300 and 0.325) were considered in this study. Details of this factorial design and designation of ECC mixtures are presented in Table 3.3

Table 3.3 ECC mixture proportions

MIX ID.	W/B	D_{max}, µm	S/B	SP/B, %	C	FA	Water	PVA	Sand	SP
					kg/m^3					
1	0.27	400	0.36	0.200	381	838	329	26	443	2.43
2	0.27	400	0.36	0.225	381	838	329	26	443	2.74
3	0.27	400	0.36	0.250	381	837	329	26	443	3.05
4	0.27	400	0.36	0.275	381	837	329	26	442	3.35
5	0.27	400	0.36	0.300	381	837	329	26	442	3.66
6	0.27	400	0.36	0.325	381	837	329	26	442	3.95
7	0.27	400	0.45	0.200	367	806	317	26	524	2.34
8	0.27	400	0.45	0.225	367	806	317	26	524	2.64
9	0.27	400	0.45	0.250	367	806	317	26	523	2.93
10	0.27	400	0.45	0.275	367	806	317	26	523	3.23
11	0.27	400	0.45	0.300	367	806	316	26	523	3.52
12	0.27	400	0.45	0.325	367	805	316	26	523	3.80
13	0.27	1000	0.36	0.200	381	838	329	26	443	2.43
14	0.27	1000	0.36	0.225	381	838	329	26	443	2.74
15	0.27	1000	0.36	0.250	381	837	329	26	443	3.05
16	0.27	1000	0.36	0.275	381	837	329	26	442	3.35
17	0.27	1000	0.36	0.300	381	837	329	26	442	3.66
18	0.27	1000	0.36	0.325	381	837	329	26	442	3.95
19	0.27	1000	0.45	0.200	367	806	317	26	524	2.34
20	0.27	1000	0.45	0.225	367	806	317	26	524	2.64
21	0.27	1000	0.45	0.250	367	806	317	26	523	2.93
22	0.27	1000	0.45	0.275	367	806	317	26	523	3.23
23	0.27	1000	0.45	0.300	367	806	316	26	523	3.52
24	0.27	1000	0.45	0.325	367	805	316	26	523	3.80
25	0.30	400	0.36	0.200	367	807	353	26	427	2.35
26	0.30	400	0.36	0.225	367	807	353	26	427	2.64
27	0.30	400	0.36	0.250	367	807	353	26	427	2.94
28	0.30	400	0.36	0.275	367	807	353	26	427	3.23
29	0.30	400	0.36	0.300	367	807	353	26	427	3.53
30	0.30	400	0.36	0.325	367	807	353	26	427	3.81
31	0.30	400	0.45	0.200	354	778	340	26	506	2.26
32	0.30	400	0.45	0.225	354	778	340	26	506	2.55
33	0.30	400	0.45	0.250	354	778	340	26	506	2.83
34	0.30	400	0.45	0.275	354	778	340	26	506	3.12
35	0.30	400	0.45	0.300	354	778	340	26	506	3.40
36	0.30	400	0.45	0.325	354	778	340	26	506	3.67

A mortar mixer with 25-liter capacity was used in preparing all ECC mixtures (Figure 3.4). Solid ingredients, Portland cement, FA, and aggregate, were first mixed

at 100 rpm for a minute. Water and HRWR admixture were then added into the dry mixture and mixed at 150 rpm for one minute and then at 300 rpm for another two minutes to produce a consistent and uniform ECC matrices (ECC without PVA fiber). Fresh (mini slump flow diameter and Marsh cone time) and rheological properties (yield stress and plastic viscosity) measurements were performed on the ECC matrix and to define the compressive strength of ECC matrix at the age of 28 days, six 50 mm cubic specimens were cast. Then, ECC mixtures were produced by using the similar mixing procedure and similar amount of ingredients as ECC matrix and PVA fiber, which was added in last and mixed at 150 rpm for an additional 3 minutes. Mini-slump flow diameter is also measured on the ECC mixtures and percent variation due to the addition of PVA fiber is defined. From each ECC mixture, six 50 mm cubic specimens were prepared for determining the compressive strength test at the age of 28 days and at least six 360 × 75 × 50 prisms were prepared for four point bending test at the age of 28 days. All specimens were demolded after 24 hours and cured in sealed plastic bags without external moisture supply at 23 ± 2 °C for 7 days (Figure 3.5). The specimens were then air cured at 50 ± 5% relative humidity, 23 ± 2 °C until the age of 28 days for testing.

Mixing of solid ingredients

Water addition

HRWR addition

Fiber addition

Figure 3.4 Production of ECC by using Hobart Type mixer

Figure 3.5 Curing of ECC specimens after production of them

3.4 Test methods for determining fresh and hardened properties

3.4.1 Tests on Fresh Concrete

3.4.1.1 Mini Slump Flow

Workability of fresh ECC mortar was evaluated by measuring the mini-slump flow deformation and marsh cone flow time. In mini-slump flow deformation test, a truncated cone mould was placed on a smooth plate, filled with mortar, and lifted upwards (Figure 3.6). The slump flow deformation was defined as the dimension of the spread when it stops flowing. The deformation was then measured in two perpendicular dimensions (maximum diameter of the spread and the diameter perpendicular to it) and the average was reported as the final diameter. During the mini-slump flow test, any segregation around the edge of spread is also recorded visually.

Figure 3.6 Mini slump tests

3.4.1.2 Marsh Cone Flow Test

The Marsh cone test was based on measuring the time necessary for the flow of a particular volume of mortar through a flow cone. A plastic funnel with a capacity of 1500 mL and an internal orifice diameter of 4.56 mm was used in this study (Figure 3.7). The cone was completely filled with ECC matrix and the bottom outlet was

then opened, allowing the mortar to flow out. Marsh cone flow time of ECC matrix was the elapsed time (t) in seconds between the opening of the bottom outlet and the time for the flow of 100 ml of grout. The marsh cone flow time of fresh ECC matrix is compared to that of water, which was 1.76 sec. It is worth to note that the fresh ECC matrices did not show any significant stability problems in the form of segregation, bleeding or sedimentation during testing as observed from visual inspection.

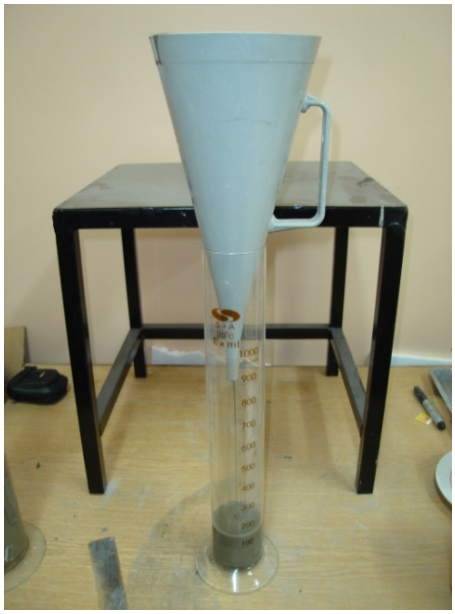

Figure 3.7 Marsh cone test

3.4.1.3 Rotational Viscometer Test

Mortar is generally considered as a non-Newtonian fluid. The rheology of fresh mortar is most often described by the Bingham model. According to this model, fresh mortar must overcome a limiting stress (yield stress) before it can flow. Once the mortar starts to flow, shear stress increases linearly with an increase in strain rate as defined by plastic viscosity. The plastic viscosity is the measure of how easily the material will flow, once the yield stress is overcome. Therefore, in order to fully describe the rheological properties of fresh mortar by the Bingham model, two parameters, namely plastic viscosity and yield stress, are necessary [Ozawa, 1989]. For that reason, it is almost impossible to define rheological characteristics of mortar by only using single conventional workability equipment [Struble, 2001]. In this experimental study, workability related fresh properties of the ECC mortar were

measured by means of mini-slump flow diameter, marsh cone flow time, and rotational viscometer.

Rheological parameters of ECC matrix (plastic viscosity and relative yield stress) were measured using a rotational viscometer with a smooth-walled concentric cylinder (Brookfield DV-II+ Pro) at 23 ± 2 °C. Viscosity of the ECC was measured at different rotational speeds (Figure 3.8). The measurements were realized at the rotational speeds range from 0 to 100 rpm, which is equal to the 34 s^{-1} shear rate. Then, the rotational speed decreased from 100 to 0 rpm. The flow curve was recorded for both the ascending and descending legs of the shear rate-shear stress. Specimens were subjected to 20 seconds for each shear rate (34 s^{-1}, 17 s^{-1}, 6.80 s^{-1}, 3.40 s^{-1}, 1.70 s^{-1}, 0.85 s^{-1}, 0.34 s^{-1} and 0.17 s^{-1}) and then shear stress were measured at each shear rate. Graph of shear rate-shear stress were drawn and plastic viscosity (slope of graph) and yield stress (the point that the line of shear rate-shear stress intersects y-axis) were calculated by assuming Bingham behavior for each ECC mixture. Rheological parameters were determined easily by linear regression

$$T = g + Nh \tag{3.1}$$

where g ($N \cdot mm$) and h ($N \cdot mm \cdot s$) are constants corresponding to yield stress and plastic viscosity, respectively. The measured relative yield stress of matrix was quite low, in fact nearly zero, and sometimes reported as negative. The physically impossible negative yield stresses were also reported by other researchers for concrete [Ferraris, 2001].

Figure 3.8 Rotational viscometer test

3.4.2 Tests on Hardened Concrete

3.4.2.1 Compressive Strength Test

Thirty six cubic samples of 50 mm were cast from each ECC mixture. The compression test was carried out on the cubic specimens by using a 3000 kN capacity testing machine in accordance with ASTM C39 (2003) (Figure 3.9). ECC cubic samples were tested for compressive strength measurement at the age of 28 days.

Figure 3.9 Compression testing machine and cubic samples

3.4.2.2 Flexural Performance

To measure the flexural performance of ECC mixture, thirty six prismatic samples (6 specimens for each age of testing) having dimensions of 360x75x50 mm were cast from each produced ECC mixture. ECC prisms were first cleaned, and then flexural strength under four-point test was performed by using universal testing system (Figure 3.10).

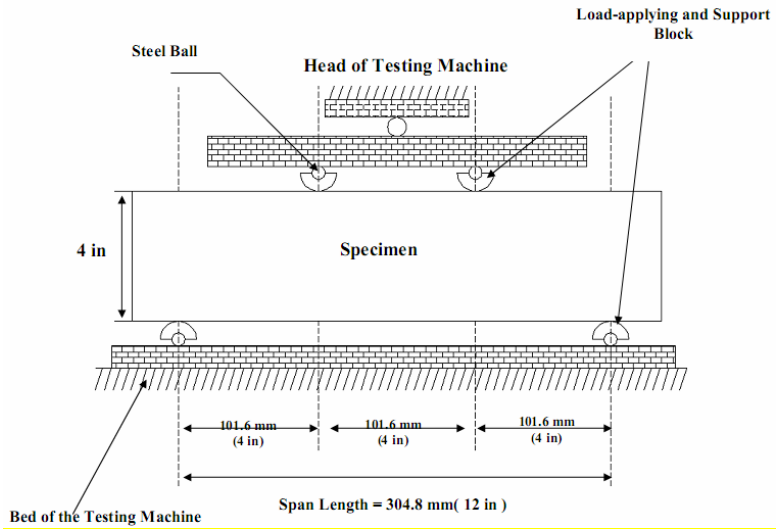

Figure 3.10 Four-point bending test setup

Four point bending test was performed on a closed-loop controlled material test system at a loading rate of 0.005 mm/s. The capacity of the loading frame was 100 kN (Figure 3.11). A four point bending loading fixture was developed to eliminate extraneous deformations such as support settlements and specimen rotations. The span length of flexural loading was 304 mm with a 101 mm center span length. During the flexural tests, the load and mid-span deflection were recorded on a computerized data recording system. Linear variable displacement transducer (LVDT) was fixed on the test set-up to measure the flexural deflection of the specimen. After bending tests, crack widths on the surface of the specimens were also measured by using a macroscope (Figure 3.12). To evaluate composite performances, microstructural analysis in terms of scanning electron microscopy (SEM) and mercury intrusion porosimetry (MIP) were also performed on selected mixtures. The results obtained from the mechanical tests and microstructural analysis at the aggregate-matrix and fiber-matrix interfaces lead to a better understanding of behavior, and may be used in the improvement of mechanical performance and ductility of ECC

Figure 3.11. Four-point Flexural Strength test machines

Figure 3.12. Control of crack widths of specimens tested by four-point test

CHAPTER IV

RESULTS AND DİSCUSSİON

4.1 Result and Discussion

4.1.1 Test Results

Table 4.1 presents the rheological parameters (plastic viscosity and yield stress), marsh cone flow time and mini slump flow diameter values of the ECC matrix and mini slump flow diameter of the ECC mixtures. Percent variation in the mini slump flow diameter due to the addition of PVA fibers is also calculated and presented in Table 4.1. Mid-span beam deflection capacity (at maximum flexural stress) and flexural strength values of ECC and compressive strength of ECC and ECC matrix are given in Table 4.2. Following sections of paper present the statistical analysis of test results and effect of each parameter, which was studied in the factorial experimental design program. Test results are evaluated and discussed by considering the analysis of variance (ANOVA) results.

4.1.2 Statistical Assessments of Test Results by Analysis of Variance (ANOVA)

ANOVA evaluates whether the independent variables (W/B, S/B, SP/B and Dmax) have an effect on the dependent variables (mini-slump flow diameter, Marsh cone flow time, yield stress, plastic viscosity, mid-span deflection, flexural and compressive strengths). It can also be used to identify whether the interactions of independent variables have an effect on the dependent variables. Sometimes, it may be difficult to analyze the effect of different factors on the variation of dependent variables; ANOVA results can be a useful tool to illustrate the effect variables have on one another [Pradhan and Bhattacharjee, 2009].

Table 4.1 Fresh properties of ECC matrix (without PVA fibers) and ECC (with PVA fibers)

Mix no	ECC matrix (ECC without PVA fibers)				ECC	Variation in mini slump flow diameter (%)
	Rheological parameters		Marsh cone flow time (seconds)	Mini slump flow diameter (mm)	Mini slump flow diameter (mm)	
	Yield stress (Pa)	Plastic viscosity (Pa.s)				
M1	3.376	1.640	-	150.0	104.5	30.3
M2	3.719	1.507	181.06	173.5	121.5	30.0
M3	3.013	1.360	178.00	227.0	126.0	44.5
M4	1.769	1.056	88.90	299.5	156.0	47.9
M5	-0.226	0.499	55.75	352.5	165.5	53.0
M6	-0.067	0.395	40.00	404.5	188.0	53.5
M7	4.882	1.534	-	96.5	90.0	6.7
M8	3.529	1.364	-	160.5	95.0	40.8
M9	3.627	1.454	302.65	176.0	103.0	41.5
M10	2.758	1.377	141.01	250.5	100.5	59.9
M11	0.267	0.803	83.20	340.0	163.0	52.1
M12	0.474	0.468	55.06	360.0	181.5	49.6
M13	3.338	1.640	-	158.0	103.0	34.8
M14	2.726	1.500	123.35	216.5	128.0	40.9
M15	1.914	1.420	73.73	276.0	145.5	47.3
M16	1.300	1.180	91.04	286.5	135.5	52.7
M17	0.978	0.641	58.87	326.5	156.5	52.1
M18	-0.083	0.331	48.46	378.5	189.5	49.9
M19	6.532	1.700	-	117.0	94.0	19.7
M20	4.872	1.431	-	144.5	97.0	32.9
M21	4.188	1.655	-	174.5	114.5	34.4
M22	4.377	1.401	272.03	191.0	102.5	46.3
M23	2.214	1.220	126.54	264.0	115.0	56.4
M24	0.527	0.683	70.53	346.0	152.5	55.9
M25	2.222	1.140	158.48	171.5	116.0	32.4
M26	1.930	1.037	118.53	204.5	148.5	27.4
M27	1.944	0.922	58.86	268.5	182.5	32.0
M28	1.005	0.582	44.72	339.0	205.0	39.5
M29	0.535	0.417	36.11	365.0	209.5	42.6
M30	-0.038	0.252	31.47	404.0	231.5	42.7
M31	2.725	1.164	-	133.0	98.0	26.3
M32	2.413	1.107	362.87	161.0	102.5	36.3
M33	2.391	1.051	126.25	205.0	122.0	40.5
M34	2.003	0.926	75.58	269.5	159.0	41.0
M35	0.903	0.585	54.71	338.5	187.0	44.8
M36	-0.248	0.455	52.25	360.0	203.5	43.5

Table 4.2 Mechanical properties of ECC matrix and ECC

Mix no	Mid-span deflection at max flexural load (mm)	Flexural strength (MPa)	Compressive strength (MPa)	
			ECC matrix (without PVA fibers)	ECC (with PVA fibers)
M1	4.25	10.29	49.64	51.25
M2	5.34	10.62	50.18	50.90
M3	6.32	10.92	51.71	53.16
M4	5.87	11.03	47.47	54.16
M5	5.64	10.93	47.10	54.39
M6	5.50	10.63	46.57	54.63
M7	3.94	10.11	44.14	46.50
M8	4.68	10.84	48.94	51.44
M9	5.36	11.42	44.99	47.46
M10	5.31	10.95	49.21	51.70
M11	5.13	10.88	45.98	46.81
M12	5.06	10.51	51.26	56.89
M13	3.41	9.59	44.29	48.16
M14	3.74	9.76	46.82	46.78
M15	4.83	9.67	47.06	47.79
M16	4.35	10.07	46.35	47.39
M17	4.40	9.52	51.81	55.27
M18	4.19	9.97	51.25	55.72
M19	2.73	9.52	46.51	45.10
M20	3.18	9.44	43.27	46.11
M21	3.52	9.76	47.95	46.25
M22	4.02	9.41	45.98	48.56
M23	3.98	9.77	51.85	51.89
M24	3.91	9.13	48.89	50.05
M25	5.07	7.83	41.85	39.35
M26	6.08	8.31	42.09	40.76
M27	6.17	8.77	41.96	42.93
M28	5.70	8.53	41.89	43.19
M29	5.05	8.22	44.37	41.64
M30	4.88	8.63	40.75	44.95
M31	4.56	7.77	38.30	39.14
M32	4.41	7.77	38.22	38.47
M33	4.96	8.10	40.19	41.60
M34	4.38	8.33	39.74	44.21
M35	4.26	8.62	42.48	42.14
M36	3.90	8.55	38.68	40.58

The test results were analyzed to find out the variation in the dependent parameters depends on the independent parameters. A statistical analysis was performed to determine the statistically significant (p-level < 0.05) independent parameters and their percentage contributions on the dependent parameters. Statistically significant linear regression models were obtained for the each dependent parameter depends on the independent parameters. Statistical analysis was performed and the models that have the p-levels less than and equal to 0.05 have accepted as the significant models. ANOVA results were presented in Table 4.3

In ANOVA study, the total sum of squares was calculated, which was partitioned into the sum of squares for individual factors and the sum of the squares for the residual random error. The mean squares of the factors were calculated by dividing their corresponding sum of squares by the associated degrees of freedom. Then, the effect of individual factors was evaluated by testing the hypothesis of equality of variances, which is the test of a null hypothesis or simply the significance test at a particular probability level. For this, the ratio of mean squares of factors to the mean squares of the residual error, i.e. F-statistic, was calculated and compared to the tabulated F-values related to Fisher distribution. The F-values related to Fisher distribution depend on the number of degrees of freedom of the individual factors, number of degrees of freedom of the residual error and the probability level [Pradhan and Bhattacharjee, 2009; Hicks, 1982]. Degree of contribution (ρ%) of each significant factor was also obtained to determine the level of its statistical importance in the model. The column under ρ% in Table 4.3 provides an idea of the degree of contribution of the independent parameters to the measured dependent parameter (test results). If the ρ% is high, the contribution of the factors to that particular response is greater. Likewise, the lower the ρ%, the lower the contribution of the factors on the dependent parameter (test results) [Srinavasan, Narasimhan and Ilango, 2003].

Table 4.3 Statistical evaluation of test results by ANOVA

Dependent parameters	Independent parameters	Regression model	R	DF	SSS	MS	F-value	P-value	S	%ρ
Mini slump flow diameter	Constant	-25.9	0.978	…	…	…	…	…	…	…
	W/B	790.9		1	4505	4506	11.5	< 0.0001	Y	1.6
	S/B	-1191.1		1	23205	23205	59.4	< 0.0001	Y	8.4
	SP/B	1947.1		1	248784	248784	636.9	< 0.0001	Y	90.0
	D_{max}	…		…	…	…	…	…	N	…
	Error	…		32	12498	386	…	…	…	…
Marsh cone flow time	Constant	912.2	0.856							
	W/B	-3820.2		1	105074	105074	7.6	0.0473	Y	8.5
	S/B	3564.6		1	207837	207837	15.0	0.0006	Y	16.9
	SP/B	-3741.3		1	918558	918558	66.1	< 0.0001	Y	74.6
	D_{max}	…		…	…	…	…	…	N	…
	Error	…		32	444750	13898	…	…	…	…
Yield stress	Constant	10.2	0.901	…	…	…	…	…	…	…
	W/B	-33.9		1	8.3	8.3	14.6	0.0006	Y	10.5
	S/B	24.9		1	10.1	10.1	17..8	0.0002	Y	12.7
	SP/B	-30.5		1	60.929	60.9	107.2	< 0.0001	Y	76.8
	D_{max}			…	…	…	…	…	N	…
	Error	…		32	18.2	0.5	…	…	…	…
Plastic viscosity	Constant	5.3	0.927	…	…	…	…	…	…	…
	W/B	-12.5		1	1.1	1.1	37.6	< 0.0001	Y	18.9
	S/B	3.7		1	0.2	0.2	7.6	0.0095	Y	3.8
	SP/B	-8.4		1	4.6	4.6	153.6	< 0.0001	Y	77.2
	D_{max}						…	…	N	
	Error	0.95		32		0.03				
Mid-span deflection at maximum flexural stress	Constant	16.7	0.800	…	…	…	…	…	…	…
	W/B	…							N	…
	S/B	-17.6		1	5.1	5.1	17.5	0.0002	Y	29.8
	SP/B	…							N	…
	D_{max}	-0.012		1	11.9	10.9	41.3	< 0.0001	Y	70.2
	Error	…		33	9.5	0.3	…	…	…	…
Flexural strength	Constant	36.8	0.986	…	…	…	…	…	…	…
	W/B	-82.5		1	36.8	36.8	400.3	< 0.0001	Y	81.9
	S/B	…			…	…	…	0.1893	N	…
	SP/B	2.8		1	0.5	0.5	5.7	0.0217	Y	1.2
	D_{max}	-0.011		1	7.6	7.6	82.9	< 0.0001	Y	17.0
	Error	…		32	2.9	0.1	…	…	…	…
Compressive strength	Constant	122.9	0.864	…	…	…	…	…	…	…
	W/B	-240.8		1	392.8	313.0	84.8	< 0.0001	Y	89.8
	S/B	-34.6		1	19.6	19.6	4.2	0.0478	Y	4.5
	SP/B	19.5		1	24.9	24.9	5.4	0.0269	Y	5.7
	D_{max}			…	…	…	…	…	N	…
	Error			32	148.3	4.6	…	…	…	…

*R: Correlation coefficient; DF: Degree of freedom; SS: Sum of squares; MS: Mean square; S: Significancy

4.2 Properties of ECC Mixtures

4.2.1 Fresh and Rheological Properties of ECC Mixtures

4.2.1.1 Mini Slump Flow Diameter

Mini-slump flow diameter test is used to evaluate the workability of ECC matrix (ECC without PVA fibers) and ECC (with PVA fibers). As seen in Table 4.1, mini slump flow diameter of the both ECC matrix and ECC increases with the increase of SP/B content irrespective of the W/B, S/B and Dmax design parameters. Gradual increase in mini slump flow diameter with the increase of SP/B ratio suggests that neither ECC matrix nor the ECC mixtures did reach to "saturation point" of the used chemical admixtures, no instability and bleeding problem was observed. As known, the saturation point is defined as the superplasticizer dosage beyond which the slump flow diameter and time do not decrease appreciably. As also seen in Table 4.3, W/B, S/B and SP/B are the significant parameters on the mini-slump flow diameter of the both ECC and ECC matrix. However, SP/B is appeared to be the most effective parameter and its percent contribution on the mini-slump flow diameter increase was around 90%. SPs are surface active agents and usages of them modify the surface charges on the cement particles and thus make them disperse [Bjormstrom and Chandra, 2004]. Contrary to the expectations, effect of W/B parameter on the variation of mini slump flow values is at very low level and its percent contribution according to the ANOVA results was around 1.6%. This may be due to the relatively narrow range (0.27 and 0.30) of W/B parameter. ANOVA results also show that increasing the S/B ratio from 0.36 to 0.45 influenced the mini-slump flow diameter around 8.4%. As also seen in Table 4.1 and as expected, with the addition of PVA fiber to the ECC matrix, mini slump flow diameter decreased remarkably.

4.2.1.2 Marsh cone test

The Marsh cone test is a workability test used for specification and quality control of cement pastes and grouts [Roussel and Roy,2005]. In present study, it is used to measure flow time of fresh ECC matrix. This measured flow time is linked with the fluidity of the ECC matrix. The longer the flow time of ECC matrix, the lower is the

fluidity. Marsh cone flow test results and their analysis of variance outcome are presented in Tables 4.1 and 4.3, respectively. As seen in Table 4.1, some ECC matrices do not have the Marsh cone flow time due to their high consistency, and increment in SP/B content and W/B ratio eliminated the high consistency and ECC matrix starts to flow its own weight and gravity force. Moreover, augmentation in S/B ratio negatively affects the fluidity of the ECC matrix and increased number of mixtures, which do not have the measured Marsh cone flow time. Consistent with the ANOVA results, fluidity of the ECC matrix soared with increase of SP/B ratio, which exhibited the greatest effect of 74.6% on the fluidity time of ECC matrix. As in mini-slump flow test results, SP/B parameter followed by the S/B and W/B parameters with the percent contribution on Marsh cone flow time of 16.9 and 8.5, respectively. It can be observed that Marsh cone flow times increase with the decrease in W/B, as expected. However, as a result of narrow studied range in experimental program, its contribution on flow time by ANOVA was appeared limited with 8.5%. As also in mini-slump flow diameter, increase of maximum aggregate size from 400 μm to 1000 μm did not significantly cause the decrease of fluidity time of ECC matrix. ANOVA results also confirmed mentioned results and Dmax parameters appeared as insignificant.

4.2.1.3 Yield stress

Yield stress is the shear stress required by a viscoelastic material for initiating a plastic deformation. It is the maximum shear stress under which the material is at rest but beyond which the material will start to flow or deform [Lu and Wang, 2010]. Lower yield stress of the ECC matrix requires less stress to initiate flow (lower yield stress generally corresponds to higher slump flow). The ECC matrix material stops flowing when the weight of the matrix is lower than the yield stress [Yang, Sahmaran and Li, 2009]. Yield stress values of the produced ECC matrix are presented in Table 4.1 and Figure 4.1. As the test results are evaluated, it can be easily seen that some ECC matrix have the negative yield stress values due to the possible measurement artifacts. Negative yield stress might occur deviations from the Bingham model and resulting in a non-linear relationship between shear stress and shear rate [De Larrard, Ferraris and Sedran, 1998; Cyr, Legrand and. Mouret,2000; Feys, Verhoeven, and Schutter, 2008]. However, in general, as seen in Figure 4.1, yield stress dropped off

remarkably with the raise of SP/B and W/B ratio irrespective of S/B and D_{max} parameters. This is mostly due to the dispersing action of the SP. In dispersing action, the polycarboxylate-based SP hinders the flocculation of cement particles and disperses them more evenly due to steric repulsion, hence enhancing the flowing ability of the binder pastes through reduced interparticle friction and greater free water content [Safiuddin, West, and Soudki,2010], therefore, lower the relative yield stress of fresh ECC mixture [Yang, Sahmaran, Yang, and Li,2009]. Increase in S/B ratio from 0.36 to 0.45 increased the yield stress values of the ECC matrix for the both W/B ratio, most probably due to the higher degree of friction and collision of solid particles, which increases the matrix shear stress and viscosity [Lu, Wang and Rudolphi, 2008]. Moreover, alteration of maximum aggregate size from 400 μm to 1000 μm slightly affects the yield stress values of the ECC matrix. The smaller the aggregate size results in higher yield stress. This agrees with the common finding that a decrease in maximum size of aggregate generally increases the water demand of the concrete [Mehta, 1993; Lu, Wang and Rudolphi,2008]. As known, be larger maximum aggregate size, surface area per unit volume, which has to be dampened by mixing water, will be smaller. However, this conclusion has a contrast with the finding of ANOVA study, Dmax parameter is not a statistically significant on the yield value of ECC matrix. ANOVA results also showed that three parameters – W/B, S/B and SP/B are the statistically significant on the yield stress values of the ECC matrix with the percent contributions of 10.5, 12.7, and 76.8, respectively.

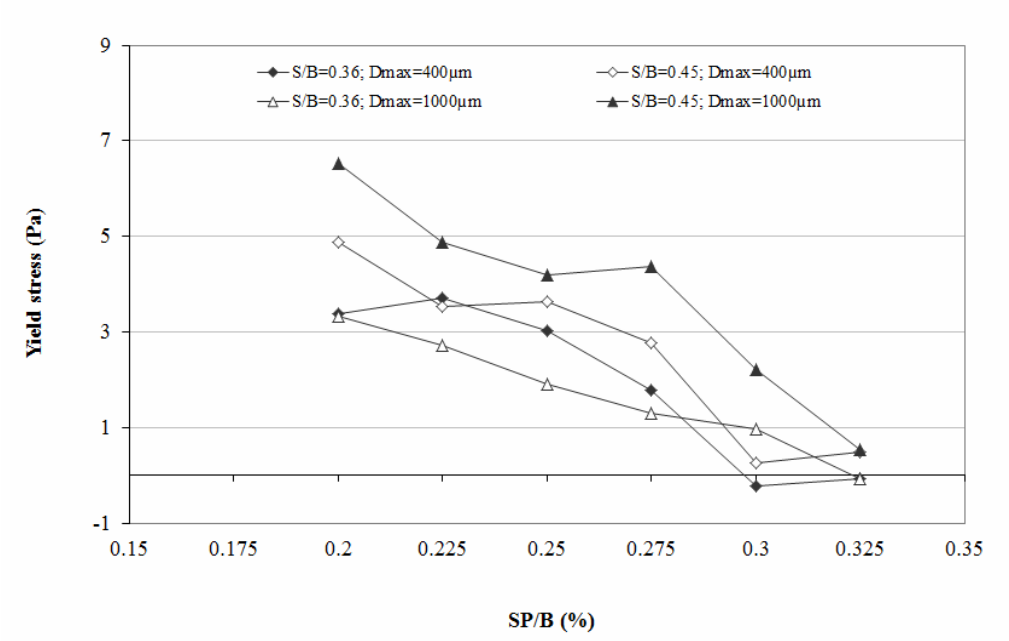

W/B = 0.27

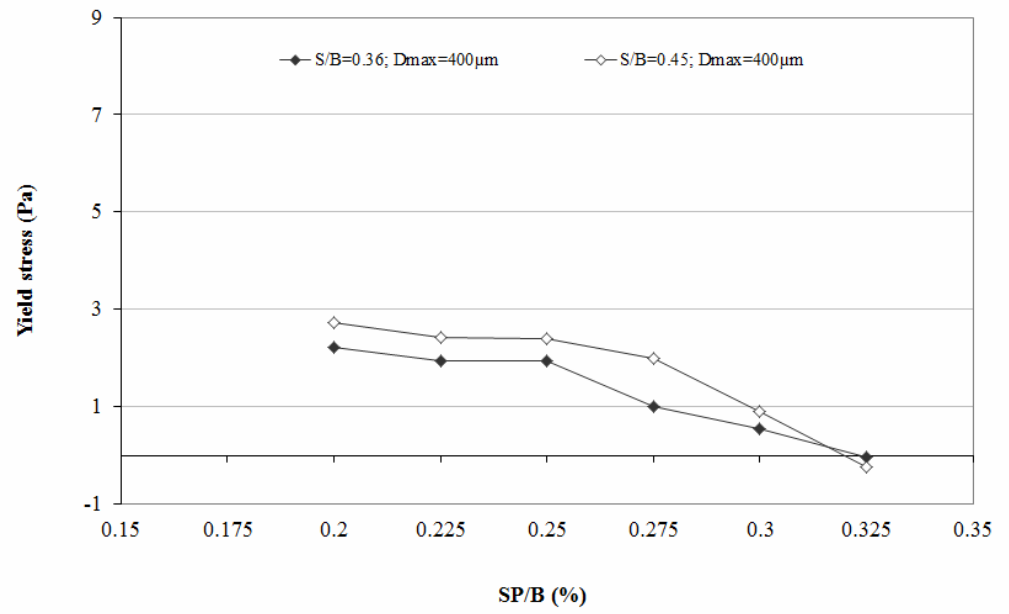

W/B = 0.30

Figure 4.1 Variation of yield stress

4.2.1.4 Plastic viscosity

Plastic viscosity controls the flowing of the ECC matrix when the matrix beaten the yield stress value. In case of self compactability of matrix, due to the addition of superplasticizers, it is known that the yield stress is much lower when compared to

traditional concrete [Feys, Verhoeven and De Schutter, 2008]. In that situation, to maintain the stability of the matrix, the plastic viscosity must be higher. For the well distribution of PVA fibers in ECC matrix, viscosity of the matrix became great importance to obtain the desired fiber bridging efficiency of PVA fiber. Plastic viscosity test results and their variance analysis are given in Tables 4.1 and 4.3, respectively. Figure 4.2 is also illustrates the variation of plastic viscosity depend on the W/B, S/B, SP/B and D_{max} parameters. As shown in Table 4.3, the plastic viscosity is influenced by, in significant order, SP/B, W/B and S/B parameters. The SP/B had the greatest effect on the plastic viscosity (77.2%). The increase in ratio of W/B had about five times greater effect than an increase in S/B ratio (18.9% vs. 3.8%). However, the increase in SP/B ratio had approximately four times greater influence than the W/B ratio on decreasing plastic viscosity of ECC matrix. Influence of SP/B ratio has deserved attention when used with low W/B ratio mixtures. As also seen in Figure 4.2, steady increase in SP/B ratio had the considerably impairment in plastic viscosity of ECC matrix regardless of W/B, S/B and D_{max} parameters. The repulsive effect, dispersion of particles and low buildup of structure formation might be responsible for the noteworthy effect of SP/B on plastic viscosity of ECC matrix. In relation to the effect of W/B ratio, the friction reduction of surface particle might be considered [Senff, Barbetta, Repette, Hotza, and Paiva, 2009]. The test results also indicate that ECC matrix viscosity increases slightly with an increase in S/B ratio but does not always increase with the augmentation of maximum aggregate size. The plastic viscosity of cement paste, as in yield stress, mini-slump flow diameter and Marsh cone flow time, is obviously a function of the superplasticizer, water, and quartz sand contents, reflected by the ratios of SP/B, W/B, and S/B parameter. Therefore, in order to obtain ECC matrix with desired flowability and target yield stress and plastic viscosity, regulation of SP/B ratio is crucial and vital.

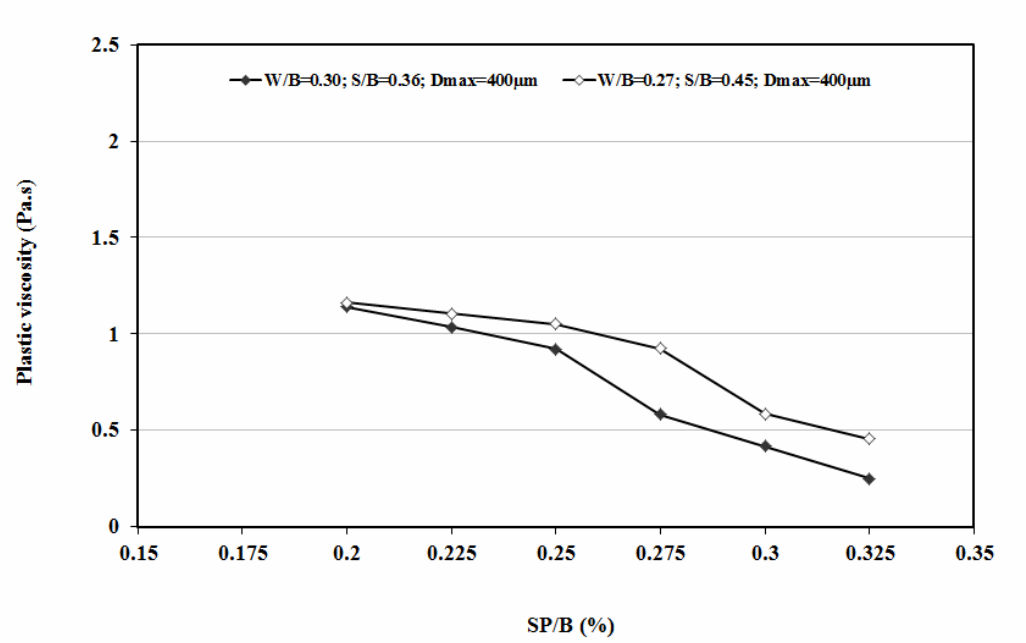

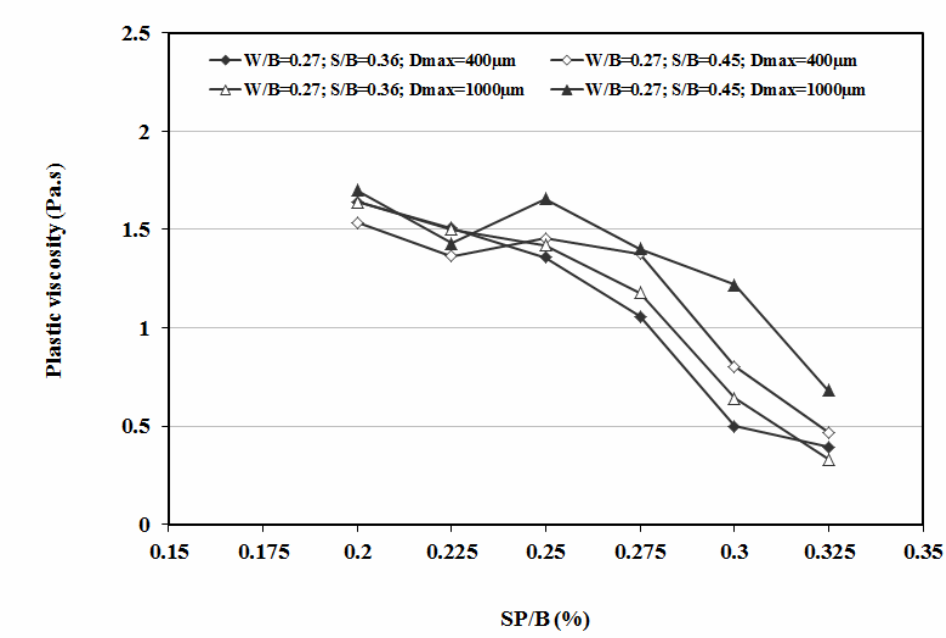

Figure 4.2 Variation of plastic viscosity

4.2.2 Hardened Properties of ECC Mixtures

4.2.2.1 Mid-span deflection

Mid-span deflection capacity of ECC mixtures, which indicates the material ductility, depend on the W/B, S/B, SP/B and D_{max} parameters are given Table 4.2 and variation of mid-span deflection values versus SP/B ratio are demonstrated in Figure 4.3. Statistical analysis of the test results is given in Table 4.3. As shown in

both Table 4.3 and Figure 4.3, mid-span deflection values varied noticeably with the change of S/B and D_{max} design parameters. Both of these two parameters negatively effect the deflection capacity of the ECC mixtures, increasing the S/B ratio from 0.36 to 0.45 and augmentation the maximum aggregate size from 400 to 1000 μm decreased the mid span deflection values at the percent contribution of 29.8 and 70.2, respectively. Mentioned diminishing effect of both S/B and D_{max} parameters on ductility might be attributed to the corresponding damage to the uniform dispersion of fibers. . The balling of fibers encouraged by relatively coarser quarts sand prevents sufficient coating of fibers by the matrix, and thus reduces the fiber-to-matrix bonding, which is an important factor influencing ductility [Soroushian, Nagi, and Hsu, 1992]. Moreover, for ECC with the higher S/B ratio, a higher degree of aggregate interlock is expected, resulting in higher matrix toughness and work-of-fracture during crack propagation. According to the micromechanical model of steady state cracking, which is essential to achieving strain hardening behavior, high matrix fracture toughness reduces the margin to develop multiple microcrackings [Li, 1997.]. Although the statistically insignificancy of the SP/B parameter on the mid-span deflection according to the ANOVA results, an optimum SP/B ratio seems to be 0.25% for the both W/B ratio (Figure 4.3). As also seen in Table 4.3, W/B ratio is statistically insignificant on the deflection capacity of the mixtures, this results contrast with the finding of the results of Yang et al. [Yang, Sahmaran, Yang, and Li, 2009]. In that study, Yang et al. mentioned that increase of W/B ratio tends to improve the tensile strain capacity of ECC mixtures. The reason behind mentioned contrast can be that the narrow design range of W/B (0.27 and 0.30) ratio in current research.

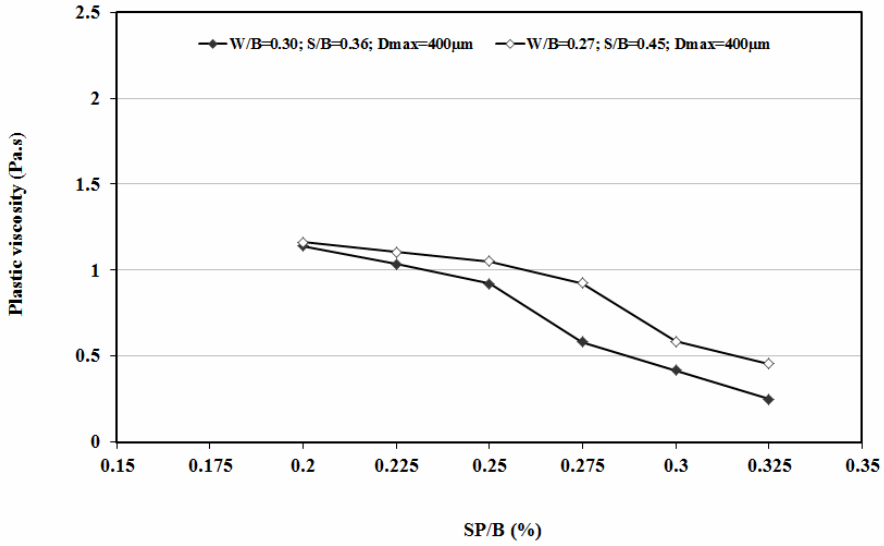

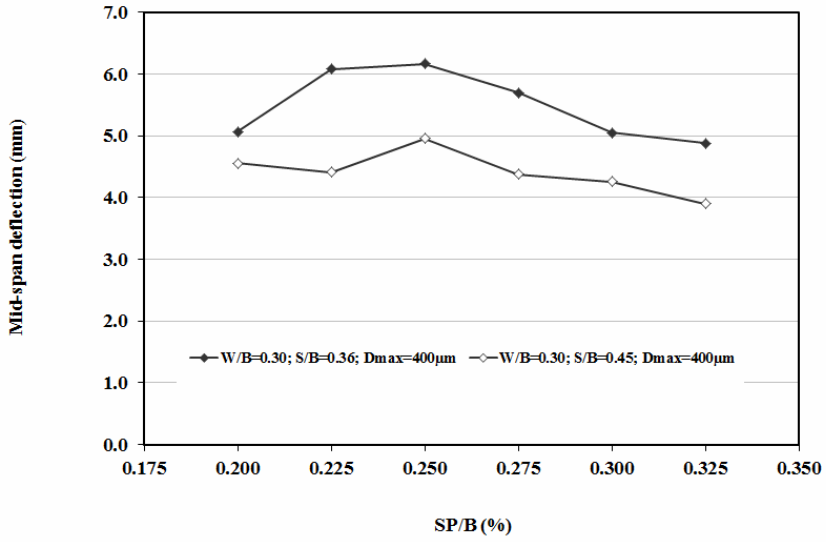

Figure 4.3 Variation of mid-span deflection values

4.2.2.2 Flexural strength

Flexural strength test results and their statistical evaluations are given in Tables 4.2 and 4.3, respectively. As seen from Table 4.2, the average ultimate flexural strengths vary from 7.77 to 11.42 MPa at age of 28 days. As shown in Table 4.3, flexural strength is influenced, in the order of contribution, by the W/B, Dmax, and SP/B.

Parameter S/B is statistically insignificant on the flexural strength variation of the ECC mixture under the limitations of current research. No distinctive variation in flexural strength depends on the S/B parameter was discernible. ANOVA results demonstrate that W/B is the most effective parameters on flexural strength with 81.9% contribution while the lowest is SP/B parameter with fairly nominal contribution (1.2%). As clearly seen in Table 4.2 and Figure 4.4, as expected, flexural strength decreases considerably as the W/B parameter increases. The increase in the W/B ratio means that there is more water between the solid particles and consequently there are more voids in hardened condition, increasing porosity and consequently leading to the decrease in the flexural strength [Haach, Vasconcelos and Lourenço2011]. The increase in maximum aggregate size (Dmax form 400 µm to 1000 µm), for any given W/B, S/B and SP/B ratio, lead to a slight reduction in the flexural strength of ECC mixtures, most probably, due to the degraded distribution of PVA fibers in the case of sand with higher maximum aggregate size.

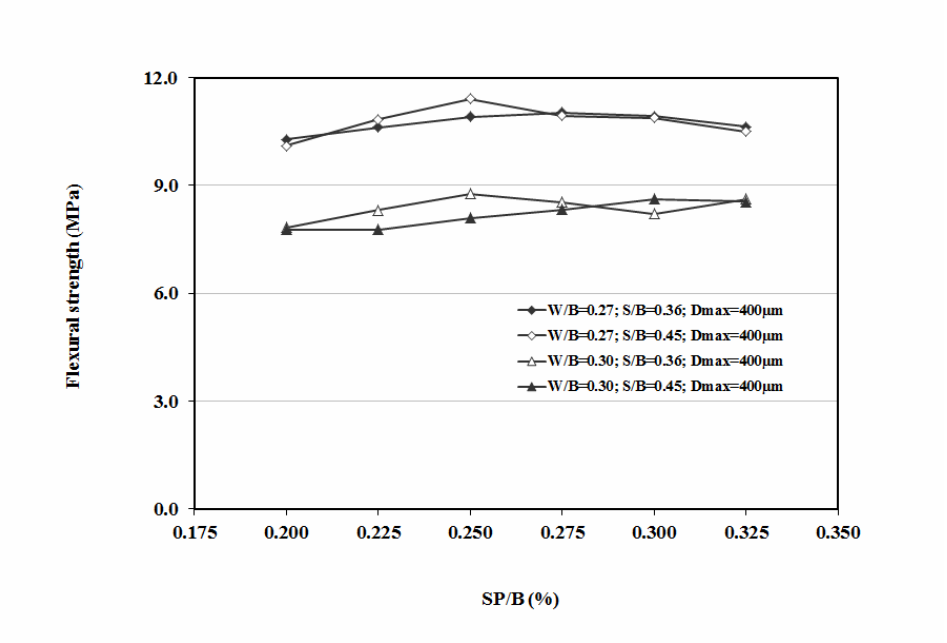

Figure 4.4 Variation of flexural strength

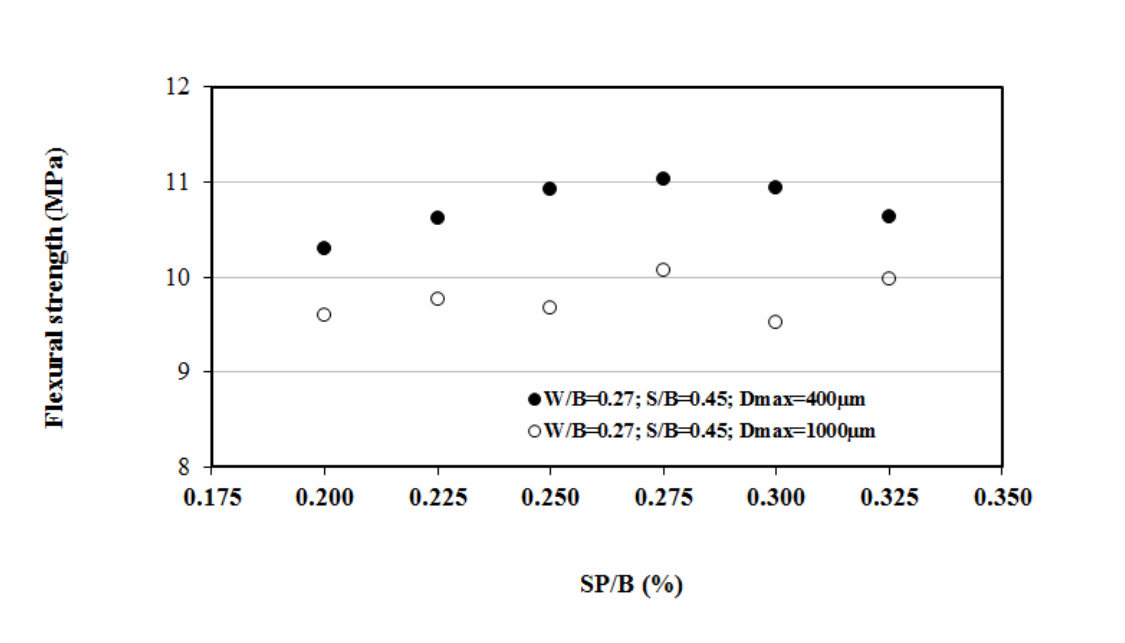

Figure 4.4 Variation of flexural strength (Cont.)

4.2.2.3 Compressive strength

The compressive strength test results of the ECC mixtures depend on the variation of W/B, S/B, SP/B and Dmax parameters are summarized in Table 4.2 and assessment of those test results by analysis of variance are given in Table 4.3. Compressive strength tests were performed on the ECC matrix and ECC specimens at 28 days of age. Six cubic specimens were tested for each mixture and average of them was presented. All ECC matrix and ECC mixtures showed compressive strengths higher than 38 MPa at 28 days of age and addition of PVA fiber to the ECC matrix did not considerably affect the test results. This value could significantly exceed that of normal concrete strength (30 MPa), and fulfill engineering requirements in most projects [Yang, Sahmaran, Yang, and Li, 2009]. As seen in Table 4.3 and as expected, W/B is the most effective parameter on the compressive strength variation of ECC specimens. Slight decrease in W/B ratio (from 0.30 to 0.27) notably increased the compressive strength and its percent contribution by ANOVA on compressive strength was around 90%. W/B has multiple role to play in cement based composites mechanical and durability properties such as decrease in W/B ratio decreases the porosity and concrete becomes more impermeable, lower W/B ratio increases the strength of composites and hence improves the its resistance to

cracking from the internal stresses that may be generated by adverse reactions [Mindess, Young and Darwin, 1981]. As seen from Table 4.2 and 4.3, an increase in the Dmax and S/B parameters had no consistent effect in the compressive strength of ECC mixtures. Statistical analysis also confirmed that Dmax is statistically insignificant on compressive strength and percent contribution of S/B parameter is 4.5. This result is contrast to the expectation, normally, compressive strength of cement based composites can be influenced by the aggregate size, smaller the aggregate size and consequently, higher surface area for a given aggregate content needs relatively higher water amount [Mehta .and Monteiro 2006.] and resulted in lower bond stress at a given load level [Cetin and Carrasquillo, 1998 However, in our case, variation of compressive strength due to the change of maximum aggregate size (Dmax) was trivial. Gradual increase in SP/B ratio did not greatly alter the compressive strength of ECC mixtures. There were no general ascending and descending trend in compressive strength due to the augmentation of SP/B ratio. Normally, it is well known that the paramount role of superplasticizer consists on a best dispersing effect of cement particles into the cement matrix by the adsorption of the chemical admixture molecules on the cement particles surface through the initial phase of hydration reactions [Chiu ,Chen and Tseng 1992;- Meddah, Zitouni and Belâabes, 2010]. This adsorption process improves the workability of the mix and reduces the water content in concrete mixture, which should improve the compressive strength [Meddah, Zitouni and Belâabes, 2010]. According to the analysis of variance, contribution of SP/B ration on compressive strength was only 5.7%.

4.3 ECC Mixture Optimization

4.3.1 Regression models

The multi linear regression models between the independent variables and the dependent responses were constructed. Before deciding the what kind of regression models (linear, quadratic, cubic etc.) are suitable for our data set, statistically significant and suggested models according to the their computed F and p-values are defined. For all the dependent variables (measured test results) only simple linear regression model was significant as follows:

$$Y = a_0 + a_1(W/B) + a_2(S/B) + a_3(SP/B) + a_4(D_{max}) + E \quad (4.1)$$

In above equation, coefficients (a_i) represent the model constants (contribution of models parameters on the measured responses) and E is random error term. The model constants are determined by multilinear regression analysis and are assumed to be normal distributed [Yahia and Khayat, 2001]. After deciding the significant model for each dependent response, insignificant parameters in significant model are then eliminated from the model. The derived models for mini slump flow diameter, Marsh cone low time, yield stress, plastic viscosity, mid-span deflection, flexural strength and compressive strength are presented with correlation coefficient values in Table 4.3. The derived models were obtained with 95% confidence interval. This signifies that there is less than 5% chance or 95% confidence limit, that the contribution of a given parameter to the tested response exceeds the value of the specified coefficient [Svermova, Sonebi and Bartos 2003]. The correlation coefficients of the proposed models for mini-slump flow diameter, Marsh cone flow time, yield stress, plastic viscosity, mid-span deflection, flexural strength and compressive strength 0.978, 0.856, 0.901, 0.927, 0.800, 0.986 and 0.864, respectively. The high correlation coefficient of most responses demonstrates excellent correlation where it can be considered that at least 95% of the measured values can be accounted for with the proposed models [Svermova, Sonebi and. Bartos 2003].

4.4 Multi-objective optimization of ECC mix proportioning

The independent parameters of the ECC mix proportions were simultaneously optimized for minimization of Marsh cone flow time and yield stress while for maximization of slump flow diameter, plastic viscosity, mid-span deflection, flexural strength and compressive strength. A numerical optimization technique using desirability functions (d_j) defined for each target response was utilized to optimize the responses [Bayramov, Tasdemir and Tasdemir 2004]. In optimization using desirability functions, the general approach is to first convert each response Y_i into an individual desirability function d_i that varies over the range, $0 \leq d_i \leq 1$ where if

response Y_i is at its target value, then $d_i=1$, and if it is outside an acceptable region, $d_i=0$. Then the design variables were chosen to maximize the overall desirability as:

$$D = (d_1 \times d_2 \times ..... \times d_m)^{1/m} \quad (4.2)$$

where m is the number of responses. A commercial statistical package was used for multi objective optimization. For simultaneous optimization in statistical package, each response must have a low and high value assigned to each goal. Moreover, the goal field for responses must be one of choices, namely, none, maximum, minimum, target, or in range [Myers and Montgomery, 2002]. Factors will always be included in the optimization, at their design range by default, or as a maximum or minimum of target goal. For the simultaneous optimization process, the factors and responses were defined as in Table 4.4.

Table 4.4 Dependent and independent parameters in the multi objective optimization problem

No	Name of dependent and independent parameters	Goal	Lower limit	Upper limit
1	W/B	In range	0.27	0.30
2	S/B	In range	0.36	0.45
3	SP/B (%)	In range	0.200%	0.325%
4	D_{max} (μm)	In range	400	1000
5	Mini-slump flow diameter (%)	Maximize	96.5	404.5
6	Marsh cone flow time (sec.)	Minimize	31.47	600
7	Yield stress (Pa)	Minimize	0	6.532
8	Plastic viscosity (Pa.s)	Maximize	0.252	1.7
9	Mid-span deflection (mm)	Maximize	2.73	6.32
10	Flexural strength (MPa)	Maximize	7.77	11.42
11	Compressive strength (MPa)	Maximize	38.22	51.25

At the end of the multi-objective optimization process, 56 different solutions which satisfied the specified constraints and limits could be obtained. The overall desirability of the functions ranged from 0.243 to 0.751. Proposed ECC mix proportions with highest desirability value of 0.751 and their expected test results are given in Table 4.5.

Table 4.5 Optimum ECC mix parameters and its expected test results

Independent and dependent parameters	
W/B	0.27
S/B	0.36
SP/B	0.303
D_{max}	400
Slump flow diameter	348.60
Marsh cone flow time	31.47
Yield stress	0.75
Plastic viscosity	0.76
Mid-span deflection	5.45
Flexural strength	10.90
Compressive strength	49.40

CHAPTER V

CONCLUSIONS

The influence of different combinations of water-binder (W/B), sand-binder (S/B), superplasticizer-binder (SP/B) ratios and maximum aggregate size (Dmax) on the fresh (mini slump flow diameter and Marsh cone time) and rheological properties (yield stress and plastic viscosity) of ECC matrices, and mechanical properties (compressive strength, flexural strength and mid-span beam deflection capacity) of ECC mixtures was investigated by means of design of experiments. The range of the parameters is as follows: 1) W/B ratio (0.27 and 0.30); 2) S/B ratio (0.36 and 0.45, by weight); 3) SP/B ratio (between 0.200 and 0.325% of binder content); 4) Dmax (400 and 1000 mm). The influence of studied parameter (W/B, S/B, SP/B and Dmax) were characterized and analyzed using ANOVA and regression models which can identify the primary factors and their interactions on the measured properties. To find out the best possible ECC mixture, under the condition of this research concept, for the desired workability and mechanical characteristics, a multi-objective optimization problem was defined and solved based on developed regression models. From the results obtained, the following conclusions can be drawn:

- W/B, S/B and SP/B are the significant parameters on the fresh and rheological properties of ECC matrices. Among these parameters, SP/B ratio is appeared to be the most effective parameter. Therefore, in order to obtain ECC matrix with desired flowability and target yield stress and plastic viscosity, regulation of SP/B ratio is crucial and vital. On the other hand, the alteration of maximum aggregate size from 400 μm to 1000 μm has slight or no effect on the fresh and rheological properties of ECC matrices.

- The mid-span beam deflection capacities, which reflect material ductility, of ECC mixtures varied noticeably with the change of S/B and Dmax design parameters. Both of these two parameters negatively affect the deflection capacity of the ECC mixtures. The other parameters have almost no effect on the mid-span beam deflection capacities of ECC mixtures.

- ANOVA results demonstrate that the W/B ratio is the most effective parameter on the flexural and compressive strength variation of ECC mixtures, while the other parameters have much less effect compared to W/B ratio.

While variations in local ingredients may be unpredictable, rheological control as described in this paper provides a relatively simple means of ensuring an ECC composite with robust tensile strength and strain capacity. The recommendations for rheological control of fresh properties in producing ECC should assist in successful adaptation of ECC using local ingredients and widely available equipment.

REFERENCES

Alaee F.J, Karihaloo B.L (2003). Retrofitting of RC beams with CARDIFRC. *ASCE J Comp Const*, 7, P. 174-186.

Ammar Yahia, KH Khayat (2001). Experimental design to evaluate interaction of high range water reducer and antiwashout admixtures in high performance cement grouts, *Cement and Concrete Research*, 31, P.749-757

ASTM Standard C39. (2003). Standard test method for compressive strength of cylindrical concrete specimens. *American society for testing and materials*. West Conshohocken, PA, USA.

Banthia, N. A., Bentur and Mufti, A(1998). Editor. *Canadian Society for Civil Engineering*, P. 64-97.

Bayramov F, Tasdemir C, Tasdemir MA. (2004). Optimization of steel fiber reinforced concretes by means of statistical response surface method. *Cement Concr Compos*; 26(6) P.665–75

Cetin, A. and Carrasquillo, R.L. (1998). High-performance concrete: Influence of coarse aggregates on mechanical properties. *ACI Material Journal*, 95, P. 252–261

Chen, B. and Liu, J. (2004). Effect of aggregate on the fracture behavior of high strength concrete. *Construction and Building Materials*, 18, P. 585- 590.

Dimitri Feys, Ronny Verhoeven, Geert De Schutter (2008). Fresh self compacting concrete, a shear thickening material, *Cement and Concrete Research* 38 P. 920–929

En-Hua Yang, Mustafa Sahmaran, Yingzi Yang, and Victor C. Li (2009). Rheological Control in Production of Engineered Cementitious Composites, *ACI Materials Journal*, V. 106, No. 4,P. 357-366]

F. De Larrard, C.F. Ferraris, T. Sedran (1998). Fresh concrete*: a Herschel–Bulkley material, Mater. Struct*. 31 P. 494–498

Ferraris C F. (1999). Measurement of the Rheological Properties of High Performance Concrete. *Journal of Research of the National Institute of Standards and Technology* 104(4) P. 461-477

Feraris, C., Kartik H.O., Russel H. (2001). The Influence of Mineral Admixture on Rheology of Cement Paste and Concrete*, Cement Concrete Research*, Vol. 31, No. 2, P.244-245

Fischer, G.S. W. and Li, V.C. (2003). Design of Engineered Cementitios Composites (ECC) for Processing and Workability Requirement. *In: BMC* 7, P. 29-36.

Gang Lu, Kejin Wang, Thomas J. Rudolphi (2008). Modeling rheological behavior of highly flowable mortar using concepts of particle and fluid mechanics, *Cement & Concrete Composites* 30 P.1–12

Gang Lu and Kejin Wang (2010). Investigation into Yield Behavior of Fresh Cement Paste: Model and Experiment, *ACI Materials Journal*, V. 107, No. 1, January-February,P. 12-19

Hicks, C.R. (1982). Fundamental Concepts in the Design of Experiments, (3rd ed.), *Rinehart and Winston, NewYork*: Holt,

Hsu KC, Chiu JJ, Chen SD, Tseng YC. (1999). Effect of addition time of a superplasticizer on cement adsorption and on concrete workability. *Cem Concr Compos;* 21(5–6) P.425–30

J. Bjormstrom z and S. Chandra (2003). Effect of superplasticizers on the rheological properties of cements, *Materials and Structures / Mat6riaux et Constructions, Vol. 36*, P. 685-692

Journal of Research of the National Institute of Standards and Technology (NIST, 1999). Measurement of the Rheological Properties of High Performance Concrete, State of the Art Report, Vol. 104, No. 5

Kim, Y.Y., Kong, H.J. and Li, V.C. (2003). Design of Engineered Cementitious Composite (ECC) suitable for wet-mix shotcreting. *ACI Materials Journal,* 100, P. 511-518.

Kong, H.J., Bike, S. and Li, V.C. (2003a). Development of a Self-Consolidating Engineered Cementitious Composite Employing Electrosteric Dispersion/Stabilization. *Journal of Cement and Concrete Composites*, 25, P. 301-309.

Kong, H.J., Bike, S. and Li, V.C. (2003b). Constitutive Rheological Control to Develop a Self-Consolidating Engineered Cementitious Composite Reinforced with Hydrophilic Poly(vinyl alcohol) Fibers. *Journal of Cement and Concrete Composites*, 25, P. 333-341.

Kunieda, M. and Rokugo, K. (2006). Recent Progress on HPFRCC in Japan. *Journal of Advanced Concrete Technology*, 4, P. 19-33.

Lacombe, P., Beaupre, D., Pouliot, N. (1999). *Rheology and Bonding Characteristics of Self-Leveling Concrete as a Repair Material, Materials and Structures*, Vol. 32, P. 593-600.

Lepech, M. and Li, V.C. (2005 a). Water Permeability of Cracked Cementitious Composites. *In: Proceeding of Eleventh International Conference on Fracture,* Turin, Italy, pp. CD-P. 4539.

Lepech, M. and Li, V.C. (2005 b). Durability and Long Term Performance of Engineered Cementitious Composites. *In Proceedings of International RELIM Workshop on HPFRCC in Structural Applications, Honolulu, Hawaii*, P. 165-174.

Li M., Li V (2009). Influence of material ductility on performance of concrete repair. *ACI Mat J*, 106, P. 419-428.

Lin, Z. and Li, V.C. (1997). Crack Bridging in Fiber Reinforced Cementitious Composites with Slip-Hardening Interfaces. *Journal of Mechanics and Physics of Solids,* 45, P. 763-787.

Lin, Z., Kanda, T. and Li, V.C. (1999). On interface property characterization and performance of fiber reinforced cementitious composites. *Concrete Science and Engineering, RILEM,* 1, 173-184.

Li, V.C. and Leung, C.K.Y. (1992). Theory of steady state and multiple cracking of random discontinuous fiber reinforced brittle matrix composites. *ASCE Journal of Engineering Mechanics*, 118, P. 2246–2264.

Li V.C. (1993). From micromechanics to structural engineering – the design of cementitious composites for civil engineering applications *JSCE J. Struc. Mech. & Earthquake Engineering*, 10 (2), P.37-48.

Li, V.C., Mishra, D.K. and Wu, H.C. (1995). Matrix Design for Pseudo Strain-Hardening Fiber Reinforced Cementitious Composites. *RILEM Journal of Materials and Structures*, 28, P. 586-595.

Li, V.C. (1997). *Engineered Cementitious Composites Tailored Composites Through Micromechanical Modeling in Fiber Reinforced Concrete: Present and the Future*,

Li, V.C, Wang, S. and Wu, C. (2001). Tensile Strain-hardening Behavior of PVA-ECC. *ACI Materials Journal*, 98, P. 483-492.

Li, V.C. (2003). On Engineered Cementitious Composites (ECC) A Review of the Material and Its Applications. *Journal of Advanced Concrete Technology,* 1, P.215-230.

Li, V.C., Lepech, M. and Li, M. (2005). Field Demonstration of Durable Link Slabs for Jointless Bridge Decks Based on *Strain-Hardening Cementitious Composites. Michigan DOT report*.

Li, V.C. (2006). Integrated Structures and Materials Design. *RILEM Journal of Materials and Structures,* P. 1-10.

Lim Y.M., Li V.C. (1997) Durable repair of aged infrastructures using trapping mechanism of engineered cementitious composites,. *Cem Concr Compos*, 19(4), P. 171-185

M. Cyr, C. Legrand, M. Mouret (2000). Study of the shear thickening effect of superplasticizers on the rheological behaviour of cement pastes containing or not mineral additives, *Cem. Concr. Res.* 30 P. 1477–1483

Markovic I., Walraven J.C., van Mier J.G.M. (2004). Tensile behaviour of high performance hybrid fibre concrete. Eds. Li et al., *Fracture Mechanics of Concrete Structures*, P. 1113-1120

Marshall, D.B. and Cox, B.N. (1988). A J-integral method for calculating steady-state matrix cracking stresses in composites. *Mechanics of Materials*, 8, P. 127–133.

Md. Safiuddin, J.S. West, and K.A. Soudki, (2010). Flowing ability of self-consolidating concrete and its binder paste and mortar components incorporating rice husk ash, *Can. J. Civ. Eng*. 37 P. 401–412

Mehta PK, Monteiro PJM. (1993) Concrete-structure, properties and materials. (2nd ed.*) Prentice-Hall*;

Mehta P.K. and Monteiro P.J.M. (2006). *Concrete*: Structure, Properties, and Materials. (3rd ed.), *McGraw Hill, New York.*

Mohammed Seddik Meddah, Salim Zitouni, Saïd Belâabes, (2010). Effect of content and particle size distribution of coarse aggregate on the compressive strength of concrete, *Construction and Building Materials* 24 P 505–512

Myers RH, Montgomery DC. (2002). Response surface methodology process and product optimization using designed experiments. *John Willey & Sons*. P. 99–103

Nicolas Roussel, Robert Le Roy (2002). The Marsh cone: a test or a rheological apparatus?, *Cement and Concrete Research* 35 2002 P 823– 830

Ozawa K, K. Maekawa, M. Kunishima, and H. Okamura (1989). Development of High Performance Concrete Based on *the Durability Design of Concrete Structures*.

Pradhan, B., and Bhattacharjee, B. (2009). Performance Evaluation of Rebar in Chloride Contaminated Concrete by Corrosion Rate, *Construction and Building Materials*, V. 23, P. 2346-2356

Proc. of the JCI international workshop on ductile fiber reinforced cementitious composites (DFRCC), (2002)

Reinhardt, H.W. and Jooss, M. (2003). Permeability and self-healing of cracked concrete as a function of temperature and crack width. *Cement and Concrete Research*, 33, P. 981-985.

Rossi P., Parant E. (2005). *Mechanical behaviours of a multi-scale fiber reinforced cement composite (MSFRCC) subjected to severe loading conditions.*

Saak, A.W., Jeninings, H.M., Shah, S.P. (2001). New Methodology for Designing Self-Compacting Concrete, *ACI Materials Journal*, Vol. 98, No. 6, P. 429-436.

Sahmaran, M. and Li, V.C. (2009). Durability Properties of Micro-Cracked ECC Containing High Volumes Fly Ash. *Cement and Concrete Research*, 39, P. 1033-1043.

Sahmaran, M. and Li,V.C. (2009). Influence of Microcracking on Water Absorption and Sorptivity of ECC. *RILEM-Journal of Materials and Structures*, 42, P. 593-603.

Soroushian, P., Nagi, M. and Hsu, J. (1992). Optimization of the use of lightweight aggregates in carbon fiber reinforced cement. *ACI Materials Journal*, 89, P. 267-276.

Srinavasan, C. B., Narasimhan, N. L., Ilango, S.V. (2003). Development of Rapid-set High Strength Cement Using Statistical Experimental Design, *Cement and Concrete Research,* V. 33, No. 9, P. 1287-1292

Struble L J, Puri U., and Ji, X. (2001) *Concrete Rheometer*. Advances in Cement Research 13(2), P. 53-63

Luciano Senff, Pedro A. Barbetta, Wellington L. Repette, Dachamir Hotza, Helena Paiva, Victor M. Ferreira, João A. Labrincha (2009). Mortar composition defined according to rheometer and flow table tests using factorial designed experiments, *Construction and Building Materials 23*, P. 3107–3111

Lucie Svermova, Mohammed Sonebi, Peter J.M. Bartos (2003). Influence of mix proportions on rheology of cement grouts containing limestone powder, *Cement & Concrete Composites 25*, P. 737–749

Tattersall, G.H., Banfill, P.F.G. (1983). The Rheology of Fresh Concrete, *Pitman Advanced Pub. Program, Boston*

Turkish Cement Manufacturers' Association (TCMA), <http://tcma.org.tr/ENG/>, (2009)

Vladimir G. Haach, Graça Vasconcelos, Paulo B. Lourenço (2011). Influence of aggregates grading and water/cement ratio in workability and hardened properties of mortars, *Construction and Building Materials* 25, P. 2980-2987

Wang, S. and Li, V.C. (2004). Tailoring of pre-existing flaws in ECC matrix for saturated strain hardening. P*roceedings of FRAMCOS-5, Vail, Colorado, USA,* P. 1005–1012.

Wang, S. and Li, V.C. (2006). High-Early-Strength Engineered Cementitious Composites. *ACI Materials Journal,* 103, P. 97-105.

Weimann, M.B.and Li, V.C. (2003). Hygral behavior of engineered cementitious composites (ECC). *International Journal for Restoration of Buildings and Monuments, 9*, P. 513-534.

Yang, E. and Li, V.C. (2006). A Micromechanical Model for Fiber Cement Optimization and Component Tailoring. In: Proceedings of *10th International Inorganic-Bonded Fiber Composites Conference, San Paulo, Brazil*, CD-Paper K4.